https://ntrs.nasa.gov/search.jsp?R=19670006062 2020-03-16T18:49:07+00:00Z

NASA CONTRACTOR REPORT

LAMINATED FERRITE MEMORY - PHASE II

PREPARED BY R. L. HARVEY
I. GORDON
A. D. ROBBI

GPO PRICE $ _____

CFSTI PRICE(S) $ _____

Hard copy (HC) 3.00

Microfiche (MF) 1.30

ff 653 July 65

FINAL TECHNICAL REPORT

Prepared under Contract No. NASw-979

RADIO CORPORATION OF AMERICA
RCA LABORATORIES
PRINCETON, NEW JERSEY

for

FACILITY FORM 602

N67 15391 (ACCESSION NUMBER)
66 (PAGES)
CR-81162 (NASA CR OR TMX OR AD NUMBER)
(THRU) 1
(CODE) 08
(CATEGORY)

NATIONAL AERONAUTICS & SPACE ADMINISTRATION • WASHINGTON, D. C. • AUGUST 1966

NOTICE

This report was prepared as an account of Government sponsored work. Neither the United States, nor the National Aeronautics and Space Administration (NASA), nor any person acting on behalf of NASA:

A.) Makes any warranty or representation, expressed or implied, with respect to the accuracy, completeness, or usefulness of the information contained in this report, or that the use of any information, apparatus, method, or process disclosed in this report may not infringe privately owned rights; or

B.) Assumes any liabilities with respect to the use of, or for damages resulting from the use of any information, apparatus, method or process disclosed in this report.

As used above, "person acting on behalf of NASA" includes any employee or contractor of NASA, or employee of such contractor, to the extent that such employee or contractor of NASA, or employee of such contractor prepares, disseminates, or provides access to, any information pursuant to his employment or contract with NASA, or his employment with such contractor.

Requests for copies of this report should be referred to

National Aeronautics and Space Administration
Office of Scientific and Technical Information
Attention: AFSS-A
Washington, D.C. 20546

LAMINATED FERRITE MEMORY - PHASE II

By

R. L. Harvey
I. Gordon
A. D. Robbi

Final Technical Report

for the period

June 1, 1965 to June 30, 1966

Distribution of this report is provided in the interest of information exchange. Responsibility for the contents resides in the author or organization that prepared it.

Prepared under Contract No. NASw-979

RADIO CORPORATION OF AMERICA
RCA Laboratories
Princeton, New Jersey

for

NATIONAL AERONAUTICS AND SPACE ADMINISTRATION

N67 15391

LAMINATED FERRITE MEMORY - PHASE II

By

R. L. Harvey
I. Gordon
A. D. Robbi

RCA Laboratories

SUMMARY

This report describes the research on thermally stable ferrite materials tailored to laminated memory arrays operated at low current levels. For this application a ferrite combining low coercive force, small grain size, high Curie temperature, and high resistivity is necessary.

The manganese-ferrous ferrite, manganese-lithium ferrite, and manganese-magnesium ferrite systems (including, in some cases, small amounts of other metal ions) are studied.

A manganese-magnesium-zinc ferrite (.10 ZnO-.27 MnO-.315 MgO-.315 Fe_2O_3) has the best combination of properties for laminated memory arrays. Arrays containing 256 x 100 conductors were successfully operated, without compensation, over a temperature range of 0°C to 50°C.

TABLE OF CONTENTS

Section		Page
I.	INTRODUCTION	1
II.	FERRITE COMPOSITIONS FOR COMPUTER APPLICATIONS	3
III.	SYNTHESIS OF FERRITE SAMPLES	5
	A. Pressed Cores	5
	B. Laminated Ferrite Arrays	6
IV.	FERRITE CHARACTERISTICS	7
	A. Magnetic Induction	7
	B. Coercive Force	23
	C. Switching Properties	24
	D. Grain Size	28
	E. Squareness	29
	F. Thermal Characteristics	30
	G. Resistivity	33
	H. Discussion	33
V.	LAMINATED FERRITE MEMORY ARRAYS	35
	A. Introduction	35
	B. Experimental Techniques	35
	C. Preliminary Data	37
	D. Operating Arrays	39
VI.	CONCLUSIONS AND RECOMMENDATIONS	42
REFERENCES		43

LIST OF ILLUSTRATIONS

Figure		Page
1	The process of spontaneous grain growth	3
2	The influence on H_c by the substitution of Co for Mn in Mn-Fe ferrite. Composition No. 26 - (.54 MnO-.46 Fe_2O_3). Composition No. 26A - (.027 CoO-.513 MnO-.46 Fe_2O_3)	23
3	Inverse switching time vs. field (Core No. 28749-94I)	25
4	Toroid switching waveform	26
5	Experimental arrangement for measuring switching speed	26
6	Inverse switching time vs. field (Core No. CW5)	27
7	The grain size of some ferrites as a function of firing temperature. Composition No. 17 - (.03 LiF-.54 MnO-.52 Fe_2O_3). Composition No. 17C - (.03 LiF-.54 MnO-.52 Fe_2O_3) + 0.25 wt. % SiO_2. Composition No. 28 - (.60 MnO-.40 Fe_2O_3) . . .	28
8	Relative magnetization as a function of ambient temperature for several ferrites of interest to this project	32
9	The change of coercive force as a function of ambient temperature for a sample of compositions No. 41 and No. 47 . . .	32
10	Experimental arrangement for measuring array operation	36
11	Memory test pulse program	36
12	Histogram of outputs for laminate samples R-31	38
13	Petrographic cross-sectional view of sample R-31	38
14	Hysteresis loop - Core No. 28749-95A	38
15	Signal output vs. temperature. Typical bit in Laminate No. 28749-97B. Switching time - 0.35 μsec	39
16	Histogram for 448 scattered bits. Laminate No. 29271-37A. Switching time - 0.25 μsec	40
17	Signal vs. ambient temperature. Laminate No. 29271-42A. Switching time - 0.2 μsec	41

I. INTRODUCTION

A. The Laminated Ferrite Memory

The laminated ferrite memory,[1] having a very rugged construction, high memory density, and fast switching at low power, is eminently suited to a space environment. Briefly, a laminated array is a monolithic sheet of ferrite with an embedded matrix of conductors. These conductors form two sets of insulated, mutually orthogonal windings. Each conductor intersection stores a binary information bit. Their operation is in a word-organized mode, with one set of windings used for read-write energization and the other set for the sense digit function. Arrays with 256-word conductors on 10-mil centers and 100 sense-digit conductors on 10-mil centers have been fabricated.

The ferrite material used in Phase I of this contract[2] had fast-switching and low-drive characteristics. However, its low Curie temperature led to excessive changes in system operating characteristics as a function of ambient temperature. The use of this material in space vehicles would therefore probably require temperature or current compensation.

The goal of the present work under the contract (Phase II) is the synthesis of a material having the desirable characteristics of the material used in Phase I, but with greatly improved thermal properties. To achieve this stability, a ferrite having a Curie temperature of at least 300°C is sought. The desired characteristics of such an improved ferrite were:

$$H_c \leq 0.5 \text{ Oe (coercive force)}$$

$$B_r \geq 1000 \text{ G (remanent flux density)}$$

$$B_r/B_m \geq 0.9 \text{ (squareness ratio)}$$

$$\rho \geq 10^6 \ \Omega\text{-cm (resistivity)}$$

$$T_c \geq 300°\text{C (Curie temperature)}$$

$$S_w \leq 0.5 \ \mu\text{sec-Oe (switching coefficient)}$$

The low coercive force (H_c) is necessitated by the limited current capability of the integrated semiconductors (e.g., MOS transistors) that drive the memory. The small switching coefficient (S_w) is used to provide element switching that is fast enough to yield reasonable signal levels and a short memory cycle time (< 3 μsec). The laminated ferrite array geometry imposes a more stringent requirement on resistivity than cores would because the embedded conductors must be electrically isolated.

During the investigation, it has become clear that one important parameter to be controlled is the grain size in the ferrite. The laminated ferrite device, toward which this entire effort is devoted, employs a ferrite plane with less than 1-mil thickness between orthogonal printed conductors. Should the ferrite grains or crystallites themselves be of this dimension (approximately

25 microns) or greater, perturbations in signal output would be likely. Therefore, grain structure ($< 10\ \mu$) is another goal of the project.

B. RCA's Approach to the Laminated Ferrite Memory

RCA's strong background on ferrites for computer applications, including thermally stable compositions, was a very valuable asset in evaluating the problems, and in establishing methods of attack, as well as in eliminating ferrite compositional systems that could not achieve the goals of the project.

The ferrite systems chosen for investigation, the problems found, the methods employed in solving them, and the results achieved during the investigation are discussed in the sections that follow. Theoretical discussions as well as experimental results are given. The compositional ferrite systems delineated in this report represent the most promising compositions capable of yielding the contract requirements. We found that the optimum values of all desired properties are not attainable in a single composition. The necessary compromises will be understood from the discussion and data presented in the report.

The ferrites were first evaluated by fabricating small pressed toroids, because they are the most useful geometry for the desired tests. As the project progressed, laminated arrays of the promising materials were fabricated and tested. The material goals of the project were essentially achieved, and 256 x 100-conductor memory arrays capable of meeting systems requirements were successfully fabricated.

The work described in this report was performed during the period June 1, 1965 to June 30, 1966 at RCA Laboratories, Princeton, New Jersey, in the Computer Research Laboratory under the general supervision of Dr. Jan A. Rajchman. Dr. Rabah Shahbender is the Project Supervisor and Mr. Robert L. Harvey is the Project Scientist. In addition to the above, the following members of RCA Laboratories' staff contributed to the project: Dr. Irwin Gordon, Mr. Robert L. Noack, Mr. Matthew R. Orlando, Dr. Anthony D. Robbi, Mr. Stephen Schor, and Mr. Chandler Wentworth.

II. FERRITE COMPOSITIONS FOR COMPUTER APPLICATIONS

Many ferrite systems are known which exhibit a rectangular hysteresis characteristic, a prime requirement for information storage in electronically alterable magnetic memories. However, the material goals of this project coupled with the structure and operating restraints of the laminated device eliminate most of these systems. For example, loop squareness may be observed in the $NiFe_2O_4$ - $NiMn_2O_4$, $NiFe_2O_4$ - $LiFe_5O_8$, and $NiFe_2O_4$ - $ZnMn_2O_4$ systems. In each case, though, the coercive force values are many times too large for low-power operation, a requirement of efficient computer memories.

For this project, a primary consideration is the thermal stability of the laminated memory. This means the use of a ferrite exhibiting a high Curie temperature. The ferrite possessing the highest Curie temperature known is $LiFe_5O_8$ (T_c = 670°C), but the coercive force of $LiFe_5O_8$ is several oersteds, much too high for this project. Of the simple ferrites (those containing a single divalent cation) that exhibit a Curie temperature of 300°C or greater, only $MnFe_2O_4$ can be prepared to have a square loop and a coercive force of less than 1 Oe for a grain size of less than 10 μ.

In earlier work at RCA Laboratories, it was found that attractive square loop properties (including low values of coercive force) can be attained when LiF is substituted for manganese ferrite. Consequently, samples with a variety of sintering temperatures were prepared of Li-Mn-Fe ferrite compositions. While the magnetic characteristics were generally good, the grain size was difficult to control. Figure 1 shows the rapid variation of grain size as a function of sintering temperature of some of these compounds. In Figure 1, (a) shows small grains obtained when the firing temperature is restricted. At a slightly higher temperature, the grains spontaneously grow to the size of the sample as shown in (c). In (b) the interesting process whereby some grains have grown to a large size at the expense of the small ones has been captured. Spontaneous grain growth led to the abandonment of lithium as a component in ferrites for the laminates. A detailed discussion of grain growth is presented in Section IV-D.

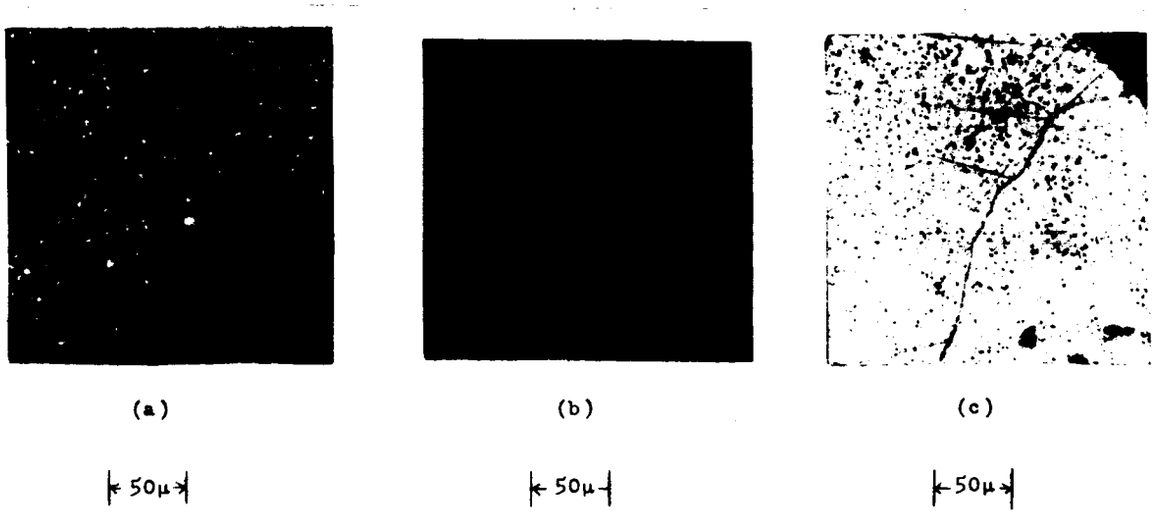

Figure 1. The process of spontaneous grain growth.

The Mn-Fe ferrite system, sintered at temperatures low enough to limit the grain size to less than 10 μ, is too high in coercive force. To reduce the crystal anisotropy (the major influence on coercive force), small substitutions of cobalt were made. Indeed, this results in a decrease in coercive force to an acceptable value for grain size less than 10 μ. Compositional changes to increase the low resistivity orders of magnitude by second-phase additives were unsuccessful. Rather, magnesium substitutions were found to be most useful; they increased the resistivity from 10^4 Ω-cm to 10^7 Ω-cm. Consequently, the system which best fulfilled the requirements is the MgO-MnO-Fe_2O_3 system.

III. SYNTHESIS OF FERRITE SAMPLES

The preparation of ferrites involves the solid-state reaction, at elevated temperatures, of the constituent ingredients. While the details of preparation have been given by many workers (e.g., Harvey, et al.[3]), the specific procedure used in this contract is described below.

A. Pressed Cores

1. The starting ingredients, such as Fe_2O_3, $MnCO_3$, LiF, etc., are weighed to supply the predetermined molar composition. All starting materials were reagent grade.*

2. The ingredients are then mixed homogeneously by ball milling, using alcohol as the vehicle.

3. The powder, after drying, is prefired (calcined) at temperatures between 800°C and 1100°C. The temperature is chosen such that the reaction between the ingredients is complete, but extensive sintering has not taken place. In all cases, the heating and cooling rate is 160°C/hour.

4. The calcined ferrite is again ball milled, using alcohol as the vehicle, for a sufficiently long time to result in a powder particle size of one micron or less. Additional mixing occurs during the grinding if the calcined material is inhomogeneous. In some instances, it is desirable to repeat the calcining and grinding steps.

5. After the ground powder is dried, it is mixed with a temporary binder suited to the subsequent pressing equipment. In the present case, 3% by weight of Flexalyn** is used because the result is a free-flowing powder well suited to the automatic molding equipment.

6. Small toroidal cores (about 0.210 cm OD, 0.135 cm ID, and 0.08 cm thickness) are formed on an automatic machine using a pressure of about 40,000 psi.

7. The cores are placed in a tube furnace for the final firing using an appropriate temperature, time, and atmosphere to result in the desired ferrite state and grain growth. In all cases the heating and cooling rate is 160°C/hour.

Pressed cores are used in all the materials exploratory work because they allow pertinent measurements to be made of the static properties, pulse switching properties, and temperature stability, as well as petrographic analysis of the grain size and structure.

---

* Fe_2O_3 - J. T. Baker, Lot 23480
$MnCO_3$ - J. T. Baker, Lot 22943
$MgCO_3$ - J. T. Baker, Lot 37188
LiF - J. T. Baker, Lot 25380
$ZnCO_3$ - J. T. Baker, Lot 21251

** Obtained from Hercules Company

B. Laminated Ferrite Arrays

The following procedure is used to fabricate 256 x 100-conductor cross-over arrays:

1. The ground ferrite powder, from step 4 above, is mixed with an organic compound consisting of Butvar,* Flexol D.O.P.,** and Tergitol non-ionic TMN** dissolved in methyl ethyl ketone. The ferrite powder and organics are milled to form a ferrite slurry.

2. The ferrite slurry is used to prepare sheets of ferrite by the "doctor-blading" techique. In this technique, the slurry is spread in an even layer on a glass substrate by the sweeping action of a blade (called a "doctor-blade") held at a constant distance above the glass surface. The bladed slurry is air-dried, resulting in a sheet of ferrite powder, held firmly together by the binder. After drying, the sheet is easily peeled from the glass surface.

3. The dry doctor-bladed ferrite sheets (cut to 1-11/16 in. x 4-3/16 in.) are embossed to form grooves which are filled with the conductor paste. One sheet has embossed lines in a lengthwise direction and one sheet has embossed lines in a crosswise direction. This arrangement, with a thin intermediate ferrite sheet, subsequently results in two sets of insulated, mutually orthogonal windings.

4. The grooves of the ferrite are filled with a platinum conductor paste.

5. The laminating of one ferrite sheet having lengthwise conductors, one blank spacer ferrite sheet, and one ferrite sheet having crosswise conductors is accomplished in a hot pressure die. This forms a compact ferrite assembly ready for the final firing.

6. The ferrite assembly, from step 5, is placed between two spaced setter plates. The assembly is heated on a hot plate (about 500°C) sufficiently long to remove the organic binder.

7. The final firing is carried out in an electric furnace having a gas tight muffle. The heating and cooling rate is 160°C per hour. The top temperature (between 1000°C and 1275°C) is held for 24 hours. The entire schedule is carried out in an atmosphere of CO_2.

At the time of the final firing of the arrays, small toroids of the same doctor-bladed material are also fired. These toroids are used to measure S_w, H_c, B, and (B_r/B_m). Also, the toroids are used for petrographic observations of the grain size and distribution. The toroids are cut from a laminate comprising three doctor-bladed sheets. The average dimensions of the sintered doctor-bladed toroids are: OD = 0.47 cm, ID = 0.33 cm, and Th = 0.018 cm.

---

* Obtained from Shawinigan Resins, Springfield, Mass.

** Obtained from Union Carbide and Chemical Corp.

IV. FERRITE CHARACTERISTICS

A. Magnetic Induction

Ferrites can be characterized by the formula $MeFe_2O_4$, where Me is a metallic cation nominally assigned a valence of $^{++}$. Fe has a nominal value of $^{+++}$, and the oxygen anion always has a valence of $^{--}$. Therefore, the formula, more accurately, may be shown as $Me^{++}Fe^{+++}{}_2O^{--}{}_4$. Moreover, the ferrites have a cubic crystal structure. The crystal is made up of a periodic distribution of cations and anions; and one can imagine a unit cell, which, when repeated in space, will reproduce the crystal. For ferrites of the type $MeFe_2O_4$, there are 8 ($MeFe_2O_4$) in a unit cell, i.e., 8 Me^{++} cations, 16 Fe^{+++} cations, and 32 O^{--} anions.

The geometrical arrangement of the 32 close-packed oxygen anions produces two types of interstices, or sites, between the anions: one, surrounded by 4 oxygen anions, is the tetrahedral site (A site), and one, surrounded by 6 oxygen anions, is the octahedral site (B site). In a ferrite unit cell, 96 sites exist between the oxygens, 64 being tetrahedral and 32 being octahedral. The cations have been found to be distributed in two ways in these sites: One with all 8 Me^{++} cations in the tetrahedral sites and 16 Fe^{+++} cations in the octahedral sites; the other with 8 Fe^{+++} cations on the tetrahedral sites, and the other 8 Fe^{+++} cations grouped with 8 Me^{++} cations in the octahedral sites.

The first distribution is called a normal ferrite, and the second distribution is called an inverse ferrite. When Me is Zn^{++} or Cd^{++}, a normal ferrite is formed. When Me is Co^{++}, Fe^{++}, Mg^{++}, Mn^{++}, Ni^{++}, or Cu^{++}, the inverse ferrite is formed. The normal spinel is not magnetic, but as will be shown, it has an important role in mixed ferrites, those of most importance to this project.

The ferrite is of course, electrically neutral; i.e., the total cation charge must equal the total anion charge. Therefore, cations of valence different from $^{++}$ or $^{+++}$ may be distributed in the oxygen interstices. This occurs for the compound $LiFe_5O_8$, where the situation ideally is $Fe^{+++}[Li^{+}_{.5}Fe^{+++}_{1.5}]O_4$. In manganese ferrite ($MnFe_2O_4$) the ionic distribution is thought to be $Mn^{++}_{.8}Fe^{+++}_{.2}[Mn^{++}_{.2}Fe^{+++}_{1.8}]O_4$ where the cations outside the brackets are on the A sites and those within the brackets are on the B sites.[4]

Each of the sublattices, referred to above as A and B sites, has a magnetization (moment) value dependent on its electronic spin configuration. In ferrimagnetic materials (ferrites) the magnetization is the result of the subtraction of the A site magnetization from the B site magnetization. Thus, a net magnetization is what is observed. Zinc has a strong preference for A sites and, when incorporated in a ferrite, the nonmagnetic Zn^{++} ion displaces Fe^{+++} and forces the iron to occupy B sites. This results in a lower moment of the A site sublattice and, consequently, an increased saturation magnetization.

The goal relating to the remanent magnetization of 1000 G or greater has been readily achieved during the experimental investigation using pressed cores. With a squareness ratio (B_r/B_m) of at least 0.90, the minimum value of saturation magnetization would be 1110 G.

The following data, from Smit and Wijn,[5] are of interest as a comparison with our experimental results:

Ferrite	$4\pi M_s$*
$FeFe_2O_4$	6000
$MnFe_2O_4$	5000
$MgFe_2O_4$	1500
$Li_{.5}Fe_{2.5}O_4$	3900

* $4\pi M_s$ is the saturation magnetization in gauss.

Two equipments are available to determine the hysteresis of toroids characteristic. One equipment automatically displays the dc hysteresis loop on an X-Y recorder. Because of the low rate of flux change and the small volume of the core, several stacked cores are linked by common windings. A 400-Hz loop tracer, requiring only a single core, is also used. The hysteresis loop is displayed on an oscilloscope and can be photographed for a permanent record. In general, the results of the two measurements are in satisfactory agreement. From the hysteresis characteristic the values of H_c, B_m, and B_r are obtained. Also, the general shape of the loop has been found to be valuable in estimating the performance of the material under pulse operation.

Referring to Table I, which shows B_m values (the magnetization for the maximum drive) for all the samples tested, there is a substantial variation of B_m as the molar composition is changed. Also, the firing temperature influences the B_m values to some extent, because of density changes.

Composition No. 19 ($MnFe_2O_4$) has a maximum B_m value of about 3900 gauss. This is in satisfactory agreement with that shown by Smit and Wijn,[5] especially when we consider that our measurements were made with a magnetizing field much lower than a saturating field.

The lowest values of B_m are found in those compositions containing a substantial fraction of $MgFe_2O_4$ (for example, Composition No. 51). Values of B_m in the order of 1700 gauss are appropriate for these compositions having a substantial concentration of nonmagnetic Mg cations on the B sites.

Data on doctor-bladed toroids are given in Table II. The B_m values for these cores are considerably less than the B_m values shown in Table I for the corresponding pressed cores. The reason for this difference is twofold. First, the density of the doctor-bladed cores is about 80 to 90% of that of pressed cores. Secondly, and more importantly, the drive field used to measure the doctor-bladed cores is considerably less than that used to measure the pressed

TABLE I

FERRITE CHARACTERISTICS – PRESSED CORES

RCA NO.	FIRING – Temp. (°C)	Time (hr.)	Atm.	ρ (Ω-cm)	H_c (Oe)	B_m (G)	B_r/B_m	S_w** (μsec-Oe)	GRAIN SIZE (Microns)	
COMPOSITION NO. 1 (.035 LiF-.515MnO-.45Fe_2O_3)										
22241-5J	1150	2	air(Q)		2.5	2970	0.94	0.41/	90%<10μ	10%-160μ
22241-5P	1250	2	air(Q)		0.27	3020	0.96	0.40/0.94	50%-160μ	50%-320μ
22241-11A	1275	2	air(Q)		0.32	3210	0.95	0.60/0.94	100%-320μ	
22241-11D	1300	2	air(Q)		0.34	2680	0.96	0.74/	100%-320μ	
COMPOSITION NO. 2 (.01LiF-.555MnO-.435Fe_2O_3)										
22241-5K	1050	2	air(Q)		1.94	2930	0.91	0.40/		
22241-5Q	1250	2	air(Q)		0.23	2800	0.98	0.73/0.73	100%-160μ	
22241-11B	1275	2	air(Q)		0.25	2510	0.95	0.75/1.75	100%-320μ	
22241-11E	1300	2	air(Q)		0.25	2550	0.92	0.64/	100%-320μ	
COMPOSITION NO. 3 (.05LiF-.54MnO-.41Fe_2O_3)										
22241-5L	1150	2	air(Q)		1.66	2640	0.93	0.48/0.48	100%<10μ	
22241-5-0	1200	2	air(Q)		0.84	2650	0.94	0.43/0.87	40%-20μ	60%-320μ
22241-5R	1250	2	air(Q)		0.51	2520	0.94	0.64/	50%-20μ	50%-320μ
22241-11F	1300	2	air(Q)		0.63	3040	0.95	0.65/	60%-40μ	40%-320μ
COMPOSITION NO. 14 (.09LiF-.50MnO-.41Fe_2O_3)										
22241-81U	1000	24	N_2	3.0×10^4		870	poor loop		100%<10μ	
22241-83G	1050	24	N_2	2.0×10^4	1.34	2000	0.80		100%<10μ	
22241-83A	1100	24	N_2	2.0×10^4	1.22	1830	0.74		75%<10μ	25%-80μ
28749-17K	1125	24	N_2	2.0×10^4	0.95	2140	0.86		50%<10μ	50%-80μ
22241-83D	1200	2	air*	10^5	0.71	2970	0.88		75%<10μ	25%-320μ
COMPOSITION NO. 15 (.07LiF-.48MnO-.45Fe_2O_3)										
22241-81V	1000	24	N_2	9×10^3		990	poor loop		100%<10μ	
22241-83H	1050	24	N_2	7.0×10^3	0.81	2350	0.88		100%-160μ	
22241-83B	1100	24	N_2	7.0×10^3	0.75	2500	0.80		100%-160μ	
28749-17L	1125	24	N_2	9.0×10^2	0.52	2520	0.92		100%-160μ	
22241-83E	1200	2	air*	10^4	1.42	2600	0.90		100%<10μ	
COMPOSITION NO. 16 (.03LiF-.48MnO-.49Fe_2O_3)										
22241-81W	1000	24	N_2	3.0×10^3		900	poor loop		100%<10μ	
22241-83I	1050	24	N_2	2.0×10^3	0.24	3020	0.97	0.67/1.2	100%-320μ	
22241-83C	1100	24	N_2	3.0×10^2	0.30	3540	0.90	0.70/1.0	100%-250μ	
28749-17H	1125	24	N_2	3.0×10^2	1.10					
22241-83F	1200	2	air*	10^4	1.22	3140	0.88		85%<10μ	15%-200μ

*Indicates that the samples were inserted into and removed from the hot furnace.
(Q) = Quenched.
**S_w values for high drive/low drive.

TABLE I (Cont'd.)

FERRITE CHARACTERISTICS – PRESSED CORES

RCA NO.	FIRING Temp. (°C)	ρ (Ω-cm)	H_c (Oe)	B_m (G)	B_r/B_m	GRAIN SIZE (Microns)	
COMPOSITION NO. 16A (.014CoO-.029LiF-.468MnO-.489Fe_2O_3)							
28749-16J	1025	3.0×10^4	1.78	3550	0.86	100%<10μ	50%-320
-17D	1035	10^4	1.51	3650	0.88	50%<10μ	50%-320μ
-16D	1050	2.0×10^3	0.22	3150	0.96	100%-320μ	
-16P	1075	2.0×10^3	0.21	3070	0.91	100%-320μ	
COMPOSITION NO. 16B (.028CoO-.029LiF-.455MnO-.489Fe_2O_3)							
28749-16K	1025	10^3	2.36	3600	0.88	100%<10μ	
-17E	1035	7.0×10^2	1.93	3680	0.90	95%<10μ	5%-80μ
-16E	1050	1.3×10^2	0.27	2880	0.88	15%<10μ	85%-320μ
-16Q	1075	1.3×10^2	0.26	3040	0.88	100%-320μ	
COMPOSITION NO. 17 (.03LiF-.45MnO-.52Fe_2O_3)							
28749-7B	1025			720	poor loop		
-7R	1035	3.0×10^2	2.00	4050	0.88	100%<10μ	
-7K	1050	10^2	0.25	3720	0.90	100%-320μ	
-7E	1075	40	0.23	3100	0.90	100%-320μ	
COMPOSITION NO. 17wCO_3 (.03Li_2CO_3-.45MnO-.52Fe_2O_3)							
28749-16L	1025		1.21	3630	0.84	100%<10μ	
-17F	1035		0.90	3850	0.86	90%<10μ	10%-160μ
-16F	1050		0.22	3210	0.83	100%-320μ	
-16R	1075		0.20	3100	0.83	100%-320μ	
-17P	1100		0.19	3340	0.80	100%-320μ	
COMPOSITION NO. 17A (.014CoO-.029LiF-.437MnO-.52Fe_2O_3)							
28749-16H	1025		1.73	3900	0.88	98%<10μ	2%-80μ
-17B	1035		1.51	4080	0.92	85%<10μ	15%-320μ
-16B	1050		0.29	3280	0.88	100%-320μ	
-16N	1075		0.24	3100	0.88	100%-320μ	
COMPOSITION NO. 17B (.028CoO-.028LiF-.424MnO-.521Fe_2O_3)							
28749-16I	1025		1.30	3880	0.79	90%<10μ	10%-160μ
-17C	1035		1.13	3700	0.83	85%<10μ	15%-160μ
-16C	1050		0.27	2900	0.74	5%<10μ	95%-320μ
-16-0	1075		0.22	3000	0.70	100%-320μ	

All firings for 24 hours in N_2.

TABLE I (Cont'd.)

FERRITE CHARACTERISTICS – PRESSED CORES

RCA NO.	FIRING Temp. (°C)	ρ (Ω-cm)	H_c (Oe)	B_m (G)	B_r/B_m	S_w (μsec-Oe)	GRAIN SIZE (Microns)	
COMPOSITION NO. 17C (.03LiF-.45MnO-.52Fe_2O_3)+0.25 wt.% SiO_2								
28749-35A	1020	10^3	1.09	3440	0.91		10%<10μ	90%-80μ
-27E	1035	10^3	0.63	3380	0.95		100%-80μ	
-27D	1050	1.7×10^3	0.61	3420	0.95		100%-80μ	
-23S	1075	1.2×10^3	0.57	3150	0.94		100%-80μ	
-27A	1125	1.2×10^3	0.53	3310	0.90		100%-80μ	
-23P	1175	10^3	0.48	3370	0.89		100%-80μ	
COMPOSITION NO. 17D (.03LiF-.45MnO-.52Fe_2O_3)+0.5 wt.% SiO_2								
28749-35B	1020	2.0×10^2	0.77	3250	0.90		20%<10μ	80%-80μ
-27F	1035	10^3	0.71	3320	0.92		50%-40μ	50%-80μ
-27-0	1050	3.0×10^3	0.71	3300	0.93		50%-40μ	50%-80μ
COMPOSITION NO. 18 (.05LiF-.41MnO-.54Fe_2O_3)								
28749-7C	1025			145	poor loop			
-7S	1035		2.32	3500	0.89		100%<10μ	
-7L	1050		0.32	3320	0.86		10%-80μ	90%-320μ
-7F	1075		0.49	3330	0.83		100%-320μ	
-7I	1100		0.37	3550	0.83		100%-320μ	
-7N	1125		0.37	3480	0.67		100%-320μ	
COMPOSITION NO. 19 (.50MnO-.50Fe_2O_3)								
28749-10A	1025	10^4	1.69	2920	0.90		100%<10μ	
-10D	1050	2.0×10^2	1.46	4250	0.90		100%<10μ	
-10G	1075	3.0×10^2	1.18	3770	0.88		100%<10μ	
-10J	1100	10^2	1.15	3170	0.92	0.50/0.61	100%<10μ	
-17I	1125	10^2	0.86	3840	0.92		100%<10μ	
-23A	1150	10^2	0.82	3740	0.91		100%<10μ	
-23L	1175	10^2	0.78	3680	0.94		90%<10μ	10%-40μ
-39A	1075*	10^3	0.94	3900	0.95		100%<10μ	
-30A	1125*	10^3	0.73	3660	0.94		95%-20μ	5%-80μ
COMPOSITION NO. 19A (.03CoO-.47MnO-.50Fe_2O_3)								
28749-7A	1025			365	poor loop			
-7Q	1035	2.5×10^3	1.21	3140	0.72	0.34/0.38	100%<10μ	
-7J	1050	3.3×10^2	1.20	3500	0.72	0.33/0.47	100%<10μ	
-7D	1075	4.0×10^2	0.61	3310	0.80	0.24/0.52	100%<10μ	
-7G	1100	3.3×10^2	0.61	3250	0.77	0.24/0.74	100%<10μ	
-7M	1125	4.0×10^3	0.53	3600	0.74	0.21/0.35	100%<10μ	
-23C	1150	3.0×10^2	0.55	3520	0.86		100%<10μ	
-23M	1175	5.0×10^2	0.80	3020	0.69		100%<10μ	
-39B	1075*	7.0×10^2	0.56	3100	0.86		100%<10μ	
-30B	1125*	7.0×10^2	0.47	3780	0.86		80%<10μ	20%-160μ

*All firings for 24 hours in N_2 (except as noted below).
28749-39A, -30A, -39B, and -30B were fired for 60 hours.

TABLE I (Cont'd.)

FERRITE CHARACTERISTICS – PRESSED CORES

RCA NO.	FIRING Temp.(°C)	ρ (Ω-cm)	H_c (Oe)	B_m (G)	B_r/B_m	GRAIN SIZE (Microns)	
COMPOSITION NO. 19B (.015CoO-.485MnO-.50Fe_2O_3)							
28749-16G	1025	3.3×10^2	1.67	3430	0.88	100%<10μ	
-17A	1035	3.3×10^2	1.37	4000	0.89	100%<10μ	
-16A	1050	3.3×10^2	1.28	3900	0.86	100%<10μ	
-16M	1075	3.3×10^2	0.98	3600	0.89	100%<10μ	
-17-0	1100	2.7×10^2	0.83	3440	0.89	90%<10μ	10%-80μ
-17J	1125	10^2	0.80	3900	0.86	90%<10μ	10%-160μ
-23B	1150	3.3×10^2	0.70	3700	0.89	90%<10μ	10%-80μ
-23N	1175	10^2	0.67	2860	0.88	90%<10μ	10%-80μ
-39C	1075*	10^3	0.83	3880	0.85	95%<10μ	5%-80μ
-30C	1125	7.0×10^2	0.65	3620	0.88	95%<10μ	5%-80μ
COMPOSITION NO. 19C (.005CuO-.495MnO-.50Fe_2O_3)							
28749-17U	1035	7.0×10^2	1.17	3470	0.87	100%<10μ	
-17Z	1050	3.3×10^2	1.47	3480	0.85	100%<10μ	
-23J	1075	1.7×10^2	1.27	3680	0.87	90%<10μ	10%-20μ
COMPOSITION NO. 19D (.005MgO-.495MnO-.50Fe_2O_3)							
28749-23T	1075	10^3	1.23	3940	0.95	100%<10μ	
-27B	1125	7.0×10^2	0.68	3780	0.92	75%<10μ	25%-80μ
-23Q	1175	3.5×10^2	0.61	3720	0.96	50%<10μ	50%-160μ
COMPOSITION NO. 19E (.015MgO-.485MnO-.50Fe_2O_3)							
28749-23U	1075	8.0×10^2	1.30	3920	0.94	90%<10μ	10%-320μ
-27C	1125	7.0×10^2	0.74	3400	0.94	60%<10μ	40%-80μ
-23R	1175	10^3	0.56	3550	0.95	50%<10μ	50%-160μ
COMPOSITION NO. 19F (.50MnO-.50Fe_2O_3)+0.1 wt.% MgO							
28749-27G	1035	7.0×10^2	1.65	3260	0.95	100%<10μ	
-27P	1050	7.0×10^2	1.46	3530	0.90	100%<10μ	
COMPOSITION NO. 19G (.50MnO-.50Fe_2O_3)+1.0 wt.% MgO							
28749-27H	1035	3.3×10^3	1.90	3650	0.91	100%<10μ	
-27Q	1050	2.3×10^3	1.70	3550	0.92	100%<10μ	
COMPOSITION NO. 19H (.50MnO-.50Fe_2O_3)+0.1 wt.% Glass							
28749-35C	1020	1.3×10^3	0.74	3500	0.93	50%-40μ	50%-80μ
-27I	1035	3.3×10^2	0.67	3700	0.91	100%-80μ	
-27R	1050	2.0×10^2	0.67	3480	0.92	100%-80μ	

*All firings for 24 hours in N_2 (except that -39C was fired for 60 hours).

TABLE I (Cont'd.)

FERRITE CHARACTERISTICS – PRESSED CORES

RCA NO.	FIRING Temp. (°C)	ρ (Ω-cm)	H_c (Oe)	B_m (G)	B_r/B_m	GRAIN SIZE (Microns)
COMPOSITION NO. 19I (.50MnO-.50Fe_2O_3)+1.0 wt.% Glass						
28749-27J	1035	10^3	1.14	3430	0.89	100%<10μ
-27S	1050	2.0×10^2	1.06	3440	0.88	100%<10μ
COMPOSITION NO. 19J (.03CoO-.47MnO-.50Fe_2O_3)+0.1 wtF MgO						
28749-35H	1035	10^3	1.00	3220	0.86	100%<10μ
-35Q	1050	7.0×10^2	0.89	4050	0.87	100%<10μ
-49S	1150	2.0×10^2	0.46	3960	0.88	95%<10μ 5%-80μ
COMPOSITION NO. 19K (.03CoO-.47MnO-.50Fe_2O_3)+1.0 wt.% MgO						
28749-35I	1035	3.0×10^3	1.50	3920	0.90	100%<10μ
-35R	1050	3.0×10^3	1.23	3760	0.90	100%<10μ
-49T	1150	7.0×10^2	0.85	3700	0.89	95%<10μ 5%-80μ
COMPOSITION NO. 19L (.03CoO-.47MnO-.50Fe_2O_3)+0.1 wt.% Glass						
28749-35J	1035	10^2	0.59	3260	0.80	100%-80μ
-35S	1050	2.0×10^2	0.56	3280	0.79	100%-40μ
COMPOSITION NO. 19M (.03CoO-.47MnO-.50Fe_2O_3)+1.0 wt.% Glass						
28749-35K	1035	10^3	1.60	3310	0.71	100%<10μ
-35T	1050	10^3	1.40	3360	0.69	100%<10μ
COMPOSITION NO. 19N (.50MnO-.50Fe_2O_3)+5.0 wt.% Glass						
28749-35L	1035	10^2	1.50	2120	0.63	100%-20μ
-35U	1050	2.0×10^2	1.34	2160	0.64	100%-20μ
COMPOSITION NO. 19-O (.0125Al_2O_3-.50MnO-.4875Fe_2O_3)						
28749-56D	1050	4.0×10^3	1.69	2900	0.90	100%<10μ
-56J	1150	8.0×10^2	0.67	3470	0.93	90%-20μ 10%-80μ
COMPOSITION NO. 20 (.01LiF-.52MnO-.47Fe_2O_3)						
28749-10B	1025	10^5	1.85	3640	0.90	100%<10μ
-10E	1050	10^4	1.65	3720	0.90	100%<10μ
-10H	1075	10^4	1.10	3550	0.90	95%<10μ 5%-80μ
-10K	1100	2.0×10^3	0.87	3760	0.90	75%<10μ 25%-80μ
-17M	1125	2.0×10^3	0.61	3270	0.94	75%<10μ 25%-160μ
-23E	1150	3.0×10^3	0.65	3360	0.95	60%<10μ 40%-160μ
-23-O	1175	2.0×10^3	0.64	3410	0.95	50%<10μ 50%-80μ
-20B	1010*	10^4	1.50	3700	0.94	100%<10μ

*All firings for 24 hours in N_2 (except that -20B was fired for 60 hours).
S_w for 10K = 0.31/0.47 μsec-Oe.

TABLE I (Cont'd.)

FERRITE CHARACTERISTICS – PRESSED CORES

RCA NO.	FIRING Temp. (°C)	ρ (Ω-cm)	H_c (Oe)	B_m (G)	B_r/B_m	GRAIN SIZE (Microns)	
COMPOSITION NO. 20A (.01LiF-.52MnO-.47Fe_2O_3)+0.1 wt.% MgO							
28749-27K	1035	2.0×10^4	1.88	3520	0.92	100%<10μ	
-27T	1050	1.7×10^4	1.69	3460	0.92	100%<10μ	
COMPOSITION NO. 20B (.01LiF-.52MnO-.47Fe_2O_3)+1.0 wt.% MgO							
28749-27L	1035	7.0×10^4	1.98	3150	0.91	100%<10μ	
-27U	1050	3.5×10^4	1.77	3180	0.94	90%<10μ	10%-160μ
COMPOSITION NO. 20C (.01LiF-.52MnO-.47Fe_2O_3)+0.1 wt.% Glass							
28749-35D	1020	7.0×10^3	0.57	3300	0.91	100%-80μ	
-27M	1035	2.0×10^3	0.49	3300	0.93	50%-80μ	50%-160μ
-27V	1050	2.0×10^3	0.46	3000	0.93	50%-80μ	50%-160μ
COMPOSITION NO. 20D (.01LiF-.52MnO-.47Fe_2O_3)+1.0 wt.% Glass							
28749-27N	1035	10^4	1.06	3420	0.90	100%<10μ	
-27W	1050	10^4	1.02	2900	0.90	100%<10μ	
COMPOSITION NO. 20E (.0288CoO-.0094LiF-.4919MnO-.4699Fe_2O_3)							
28749-35G	1035	1.3×10^4	1.14	3370	0.88	100%<10μ	
-35P	1050	10^4	1.00	4140	0.90	100%<10μ	
COMPOSITION NO. 20F (.01LiF-.52MnO-.47Fe_2O_3)+5.0 wt.% Glass							
28749-35M	1035	2.0×10^3	1.20	2020	0.74	100%-20μ	
-35V	1050	2.2×10^3	1.14	2380	0.70	100%-20μ	
COMPOSITION NO. 21 (.03LiF-.50MnO-.47Fe_2O_3)							
28749-10C	1025	10^5	2.16	3270	0.90	100%<10μ	
-10M	1035	7.0×10^3	0.91	3030	0.95	50%<10μ	50%-320μ
-10F	1050	7.0×10^3	0.29	3000	0.93	5%<10μ	95%-320μ
-10I	1075	3.3×10^3	0.25	3100	0.95	100%-320μ	
-10L	1100	3.3×10^3	0.26	3040	0.94	100%-320μ	
COMPOSITION NO. 22 (.01LiF-.48MnO-.51Fe_2O_3)							
28749-17Q	1035	3.3×10^2	1.80	3940	0.91	100%<10μ	
-17V	1050	2.2×10^2	1.50	3860	0.89	75%<10μ	25%-80μ
-23F	1075	10^2	0.70	3440	0.94	30%<10μ	70%-320μ
COMPOSITION NO. 23 (.01LiF-.49MnO-.50Fe_2O_3)							
28749-17R	1035	10^3	1.80	3800	0.91	90%<10μ	10%-160μ
-17W	1050	7.0×10^2	1.60	3720	0.90	85%<10μ	15%-160μ
-23G	1075	3.3×10^2	0.93	3270	0.93	50%<10μ	50%-160μ
All firings for 24 hours in N_2.							

TABLE I (Cont'd.)

FERRITE CHARACTERISTICS – PRESSED CORES

RCA NO.	FIRING Temp. (°C)	ρ (Ω-cm)	H_c (Oe)	B_m (G)	B_r/B_m	GRAIN SIZE (Microns)	
COMPOSITION NO. 24 (.01LiF-.50MnO-.49Fe_2O_3)							
28749-17S	1035	2.7×10^3	1.86	3520	0.90	100%<10μ	
-17X	1050	1.7×10^3	1.65	3700	0.92	100%<10μ	
-23H	1075	1.7×10^3	1.08	3200	0.91	70%<10μ	30%-320μ
COMPOSITION NO. 25 (.01LiF-.51MnO-.48Fe_2O_3)							
28749-17T	1035	5.0×10^3	1.78	3510	0.89	100%<10μ	
-17Y	1050	3.3×10^3	1.60	2860	0.92	80%<10μ	20%-80μ
-23I	1075	1.7×10^3	1.10	3170	0.93	50%<10μ	50%-320μ
COMPOSITION NO. 26 (.54MnO-.46Fe_2O_3)							
28749-49A	1050	2.2×10^4	1.63	3140	0.92	100%<10μ	
-49G	1100	2.0×10^4	1.29	3350	0.95	100%<10μ	
-49M	1150	10^4	1.01	3350	0.93	100%<10μ	
-49U	1150*	6.0×10^4	0.99	3060	0.93	100%<10μ	
-58M	1200	4.0×10^3	0.75	3500	0.95	80%<20μ	20%-80μ
COMPOSITION NO. 26A (.027CoO-.513MnO-.46Fe_2O_3)							
28749-49D	1050	1.2×10^4	0.63	3850	0.69	100%<10μ	
-49J	1100	10^4	0.49	3840	0.72	100%<10μ	
-49P	1150	9.0×10^3	0.35	3670	0.78	100%<10μ	
-49X	1150*	1.8×10^4	0.56	2820	0.75	100%<10μ	
-58N	1200	2.5×10^3	0.28	3300	0.83	98%<20μ	2%-40μ
COMPOSITION NO. 26B (.023Al_2O_3-.54MnO-.437Fe_2O_3)							
28749-56E	1050	5.0×10^4	1.79	3020	0.91	100%<10μ	
-56K	1150	3.0×10^4	0.72	3110	0.93	95%<20μ	5%-80μ
-56U	1150*	4.5×10^3	0.89	2860	0.93	75%<20μ	25%-80μ
-58-O	1200	3.6×10^3	0.61	2990	0.95	85%<25μ	15%-160μ
COMPOSITION NO. 26C (.54MnO-.46Fe_2O_3)+1.0 wt.% MgO							
28749-56M	1150	7.0×10^4	0.98	2600	0.94	100%<10μ	
-56W	1150*	5.0×10^4	1.20	2970	0.90	100%<10μ	
-58P	1200*	4.0×10^4	0.85	2920	0.94	100%<10μ	
COMPOSITION NO. 26D (.54MnO-.46Fe_2O_3)+5.0 wt.% MgO							
28749-56N	1150†	10^5	1.35	2460	0.92	100%<10μ	
-56X	1150*	3.0×10^4	1.61	3770	0.89	100%<10μ	
-58G	1200*	3.0×10^4	1.16	2730	0.95	95%<10μ	5%-40μ

All firings were for 24 hours in N_2 except as noted below.
Cores indicated by * were fired for 24 hours in CO_2.
Cores marked by † were fired for 60 hours in N_2.

TABLE I. (Cont'd.)

FERRITE CHARACTERISTICS – PRESSED CORES

RCA NO.	FIRING Temp. (°C)	ρ (Ω-cm)	H_c (Oe)	B_m (G)	B_r/B_m	GRAIN SIZE (Microns)	
COMPOSITION NO. 26E (.027CoO-.51MnO-.46Fe_2O_3)+1.0 wt.% MgO							
28749-93A	1100*	10^4	0.47	3440	0.88	95%<10μ	5%-160μ
-93E	1135*	2.0×10^4	0.34	3140	0.87	95%<10μ	5%-40μ
-58A	1150*	9.0×10^3	0.62	3510	0.90	100%<20μ	
-56-O	1150†	10^4	0.46	3400	0.91	98%<10μ	2%-80μ
-58R	1200*	3.0×10^3	0.44	3630	0.91	100%<20μ	
COMPOSITION NO. 26F (.027CoO-.51MnO-.46Fe_2O_3)+5.0 wt.% MgO							
28749-56P	1150†	10^4	0.97	3120	0.94	95%<10μ	5%-160μ
-58B	1150*	3.6×10^3	1.10	3150	0.95	100%<10μ	
-58S	1200*	4.0×10^3	0.70	2920	0.95	95%<20μ	5%-160μ
COMPOSITION NO. 26G (.014CoO-.526MnO-.46Fe_2O_3)							
28749-83R	1050	1.8×10^4	0.54	3140	0.92	50%-80μ	50%-160μ
-76B	1200	4.0×10^3	0.37	3420	0.92	60%<20μ	40%-160μ
COMPOSITION NO. 26H (.01Bi_2O_3-.54MnO-.45Fe_2O_3)							
28749-83-O	1050	1.2×10^4	0.63	3300	0.95	100%-50μ	
-83L	1080	2.3×10^5	0.57	3220	0.95	100%-40μ	
COMPOSITION NO. 26I (.005Bi_2O_3-.54MnO-.455Fe_2O_3)							
28749-83P	1050	1.7×10^4	1.76	3400	0.92	90%<10μ	10%-50μ
-83M	1080	2.0×10^5	0.75	2850	0.95	100%-30μ	
COMPOSITION NO. 26J (.03Bi_2O_3-.54MnO-.43Fe_2O_3)							
28749-83Q	1050	2.3×10^4	0.28	2650	0.95	100%-50μ	
-83N	1080	2.0×10^5	0.36	3060	0.95	100%-50μ	
COMPOSITION NO. 27 (.57MnO-.43Fe_2O_3)							
28749-49B	1050	4.0×10^4	1.6	2930	0.90	100%<10μ	
-49H	1100	4.5×10^4	1.3	3060	0.89	100%<10μ	
-49N	1150	2.0×10^4	1.0	3000	0.90	100%<10μ	
-49V	1150*	4.0×10^4	1.0	2950	0.90	100%<10μ	
-59T	1200	1.2×10^4	0.72	2880	0.91	90%<20μ	10%-160μ
COMPOSITION NO. 27A (.0255CoO-.5445MnO-.43Fe_2O)							
28749-49E	1050	3.0×10^4	1.33	3200	0.70	100%<10μ	
-49K	1100	2.0×10^4	1.13	3300	0.77	100%<10μ	
-49Q	1150	1.5×10^4	0.95	3150	0.68	100%<10μ	
-49Y	1150*	3.0×10^4	0.97	2950	0.75	100%<10μ	
-58U	1200*	7.5×10^3	0.59	3180	0.79	90%<20μ	10%-80μ

All firings were for 24 hours in N_2 except as noted below.
Cores indicated by * were fired for 24 hours in CO_2.
Cores marked by † were fired for 60 hours in N_2.

S_w Values { 56-O...0.28/0.28; 83L ... 0.47/0.55; 83M ... 0.43/0.43; 83N ... 0.49/0.70 } μsec-Oe

TABLE I (Cont'd.)

FERRITE CHARACTERISTICS – PRESSED CORES

RCA NO.	FIRING Temp. (°C)	ρ (Ω-cm)	H_c (Oe)	B_m (G)	B_r/B_m	GRAIN SIZE (Microns)	
COMPOSITION NO. 27B (.0215Al_2O_3-.57MnO-.4085Fe_2O_3)							
28749-56F	1050	10^5	1.6	3040	0.92	100%<10μ	
-56L	1150†	4.5×10^4	0.82	2730	0.92	95%-20μ	5%-80μ
-56V	1150*	10^4	0.95	2790	0.91	100%<15μ	
-58V	1200	1.2×10^4	0.63	2640	0.94	90%<30μ	10%-160μ
COMPOSITION NO. 28 (.60MnO-.40Fe_2O_3)							
28749-49C	1050	5.0×10^4	1.50	2760	0.83	100%<10μ	
-49I	1100	6.0×10^4	1.16	2900	0.85	100%<10μ	
-49-O	1150	6.0×10^4	0.89	2820	0.91	100%<10μ	
-49W	1150*	6.0×10^4	0.86	2810	0.88	100%<10μ	
-58W	1200	2.0×10^4	0.62	2580	0.93	100%<30μ	
COMPOSITION NO. 28A (.024CoO-.576MnO-.40Fe_2O_3)							
28749-49F	1050	4.5×10^4	1.75	2820	0.73	100%<10μ	
-49L	1100	5.0×10^4	1.46	2980	0.76	100%<10μ	
-49R	1150	4.0×10^4	1.21	2940	0.66	100%<10μ	
-49Z	1150*	4.5×10^4	1.24	2550	0.80	100%<10μ	
-58X	1200	2.0×10^4	0.78	3000	0.84	95%<30μ	5%-80μ
COMPOSITION NO. 28B (.60MnO-.40Fe_2O_3)+1.0 wt.% MgO							
28749-93B	1100††	5.0×10^4	0.93	2540	0.91	100%<10μ	
-91B	1150††	6.0×10^4	0.82	3220	0.93	100%<20μ	
-76A	1200*	4.0×10^4	0.71	2840	0.93	100%<20μ	
COMPOSITION NO. 29 (.05ZnO-.51MnO-.44Fe_2O_3)							
28749-56A	1050	9.0×10^4	1.33	3400	0.91	100%<10μ	
-56Q	1150	4.0×10^3	0.76	3230	0.95	100%<10μ	
-56G	1150†	1.7×10^4	0.71	3480	0.94	95%<10μ	5%-80μ
-58Y	1200*	4.0×10^3	0.50	3400	0.95	90%<20μ	10%-80μ
COMPOSITION NO. 30 (.05ZnO-.55MnO-.40Fe_2O_3)							
28749-56B	1050	1.7×10^5	1.26	3070	0.89	100%<10μ	
-56R	1150*	1.5×10^4	0.77	2730	0.90	100%<15μ	
-56H	1150†	3.0×10^4	0.70	3000	0.92	100%<15μ	
-58Z	1200	1.2×10^4	0.52	2900	0.94	90%<30μ	10%-80μ
COMPOSITION NO. 31 (.05ZnO-.57MnO-.38Fe_2O_3)							
28749-56C	1050	10^5	1.26	2770	0.90	100%<10μ	
-56S	1150*	3.0×10^4	0.76	2780	0.92	100%<10μ	
-56I	1150†	7.0×10^4	0.70	2700	0.90	100%<10μ	
-58AA	1200*	10^6	0.51	2710	0.93	95%<30μ	5%-80μ

All firings were for 24 hours in N_2 except as noted below.
Cores indicated by * were fired for 24 hours in CO_2.
Cores marked by † were fired for 60 hours in N_2.
Cores marked by †† were fired for 60 hours in CO_2.

S_w Values { 76A...0.51/0.51
561 ...0.47/0.55

TABLE I (Cont'd.)

FERRITE CHARACTERISTICS – PRESSED CORES

RCA NO.	FIRING Temp. (°C)	ρ (Ω-cm)	H_c (Oe)	B_m (G)	B_r/B_m	GRAIN SIZE (Microns)
COMPOSITION NO. 35 (.05ZnO-.49MnO-.46Fe_2O_3)						
28749-79S	1050	3.0×10^5	1.6	3600	0.90	100%<10μ
-79G	1100	1.2×10^5	0.20	2990	0.91	80 to 160μ
-79A	1125	1.7×10^5	0.21	3020	0.91	80 to 160μ
-76F	1200	5.0×10^4	0.24	2780	0.83	100%-80μ
COMPOSITION NO. 36 (.10ZnO-.44MnO-.46Fe_2O_3)						
28749-79H	1100	4.0×10^5	0.85	3100	0.84	60%<10μ 40%-80μ
-79B	1125	2.0×10^5	0.19	2820	0.85	80 to 160μ
-76G	1200	6.0×10^4	0.19	2680	0.85	40 to 160μ
COMPOSITION NO. 37 (.15ZnO-.39MnO-.46Fe_2O_3)						
28749-79I	1100	5.0×10^5	0.95	3000	0.80	95%<10μ 5%-80μ
-79C	1125	2.0×10^5	0.17	2560	0.80	40 to 80μ
-76H	1200	10^5	0.14	2190	0.86	80 to 160μ
COMPOSITION NO. 38 (.10MgO-.44MnO-.46Fe_2O_3)						
28749-79J	1100	5.0×10^5	2.10	2920	0.92	100%<10μ
-79D	1125	2.0×10^5	0.77	2710	0.94	50%<10μ 50%-160μ
-76I	1200	6.0×10^4	0.33	2580	0.92	160 to 300μ
COMPOSITION NO. 39 (.20MgO-.34MnO-.46Fe_2O_3)						
28749-79K	1100	4.0×10^5	5.3	2540	0.89	100%<10μ
-79E	1125	10^6	3.0	2800	0.93	100%<10μ
-79J	1200	3.0×10^5	0.39	2340	0.97	80 to 160μ
COMPOSITION NO. 40 (.30MgO-.24MnO-.46Fe_2O_3)						
28749-79L	1100	3.0×10^6	7.1	1900	0.90	100%<10μ
-79F	1125	7.0×10^5	4.8	2250	0.91	100%<10μ
-76K	1200	6.0×10^5	2.1	1950	0.94	100%<10μ
-92G	1250	10^5	0.46	2280	0.95	80 to 160μ
COMPOSITION NO. 41 (.40MgO-.20MnO-.40Fe_2O_3)						
28749-79T	1100	6.0×10^6	4.75	1600	0.85	100%<10μ
-79M	1150	10^7	3.0	1860	0.90	100%<10μ
-84A	1150*	1.3×10^8	4.5	1100	0.90	100%<10μ
-83A	1200	3.3×10^7	2.4	1910	0.89	100%<10μ
-83G	1250	2.5×10^6	1.1	1670	0.93	100%<20μ

All firings were for 24 hours in CO_2 except one marked * which was carried out in an atmosphere of 40 parts N_2 and 1 part O_2.

TABLE I (Cont'd.)

FERRITE CHARACTERISTICS – PRESSED CORES

RCA NO.	FIRING Temp. (°C)	ρ (Ω-cm)	H_c (Oe)	B_m (G)	B_r/B_m	GRAIN SIZE (Microns)
COMPOSITION NO. 41A (.01CoO-.39MgO-.20MnO-.40Fe_2O_3)						
28749-90I	1200	1.7×10^7	2.1	2120	0.90	100%<10μ
-92A	1250	7.0×10^6	1.8	2300	0.86	100%<10μ
-92H	1275	5.0×10^6	1.7	1890	0.75	100%<15μ
COMPOSITION NO. 41B (.03CoO-.37MgO-.20MnO-.40Fe_2O_3)						
28749-90J	1200	1.2×10^7	2.1	2200	0.73	100%<10μ
-92B	1250	6.0×10^6	2.3	1980	0.75	100%<10μ
COMPOSITION NO. 42 (.36MgO-.28MnO-.36Fe_2O_3						
28749-79V	1100	2.7×10^7	3.9	1650	0.86	100%<10μ
-79N	1150	2.0×10^7	2.6	1980	0.90	100%<10μ
-84B	1150*	1.2×10^8	3.3	1960	0.89	100%<10μ
-83B	1200	3.3×10^7	2.1	2090	0.90	100%<10μ
-83H	1250	4.0×10^6	1.0	2040	0.94	100%<20μ
COMPOSITION NO. 42A (.01CoO-.35MgO-.28MnO-.36Fe_2O_3)						
28749-90K	1200	3.0×10^7	1.7	2060	0.93	100%<10μ
-92C	1250	1.6×10^7	1.5	2020	0.80	100%<10μ
-92I	1275	10^7	1.4	2080	0.62	100%<15μ
COMPOSITION NO. 42B (.03CoO-.33MgO-.28MnO-.36Fe_2O_3)						
28749-90L	1200	3.0×10^7	1.6	2440	0.80	100%<10μ
-92D	1250	1.5×10^7	2.0	2000	0.66	100%<10μ
COMPOSITION NO. 43 (.05ZnO-.10MgO-.39MnO-.46Fe_2O_3)						
28749-79V	1100	2.0×10^5	1.60	3350	0.94	100%<10μ
-79-O	1150	1.8×10^4	0.30	2930	0.95	10 to 300μ
-83C	1200	3.0×10^4	0.32	2840	0.94	40 to 160μ
COMPOSITION NO. 44 (.05ZnO-.20MgO-.29MnO-.46Fe_2O_3)						
28749-79W	1100	10^5	2.94	2680	0.91	100%<10μ
-79P	1150	5.0×10^4	1.93	2940	0.90	100%<10μ
-83D	1200	4.0×10^4	0.52	2460	0.96	80 to 300μ
-83I	1250	1.7×10^4	0.37	2580	0.96	100%-80μ
COMPOSITION NO. 44A (.05CdO-.20MgO-.29MnO-46Fe_2O_3)						
28749-83S	1050	5.0×10^3	5.5	2630	0.90	100%<10μ
-90A	1100	5.0×10^3	2.9	2500	0.94	100%<10μ
-90E	1160	3.0×10^3	2.3	2650	0.94	100%<10μ

All firings were for 24 hours in CO_2 except one marked * which was carried out in an atmosphere of 40 parts N_2 and 1 part O_2.

TABLE I (Cont'd.)

FERRITE CHARACTERISTICS – PRESSED CORES

RCA NO.	FIRING Temp. (°C)	ρ (Ω-cm)	H_c (Oe)	B_m (G)	B_r/B_m	GRAIN SIZE (Microns)
COMPOSITION NO. 45 (.05ZnO-.30MgO-.19MnO-.46Fe_2O_3)						
28749-79X	1100	10^5	4.15	1940	0.89	100%<10μ
-79Q	1150	2.0×10^4	2.21	2680	0.87	100%<10μ
-83E	1200	1.2×10^4	2.01	2460	0.91	100%<10μ
-83J	1250	3.0×10^3	0.42	1870	0.81	100%-80μ
COMPOSITION NO. 45A (.05CdO-.30MgO-.19MnO-.46Fe_2O_3)						
28749-83T	1050	1.5×10^3	8.9	1720	0.85	100%<10μ
-90B	1100	10^3	3.6	2380	0.94	100%<10μ
-90F	1160	3.0×10^3	2.8	2620	0.92	100%<10μ
COMPOSITION NO. 46 (.10ZnO-.25MgO-.19MnO-.46Fe_2O_3)						
28749-79Y	1100	3.0×10^4	2.70	2560	0.90	100%<10μ
-79R	1150	10^4	1.38	2980	0.90	100%<10μ
-83F	1200	3.0×10^4	0.68	2300	0.95	50%<10μ 50%-80μ
-83K	1250	1.5×10^4	0.55	2800	0.48	100%-80μ
COMPOSITION NO. 47 (.05ZnO-.38MgO-.19MnO-.38Fe_2O_3)						
28749-83U	1050	1.5×10^8	6.8	1730	0.75	100%<10μ
-90C	1100	10^7	2.7	2000	0.92	100%<10μ
-90G	1160	10^6	2.0	2310	0.89	100%<10μ
-92E	1250	8.0×10^6	1.3	1950	0.91	100%<10μ
-92J	1275	1.5×10^7	1.2	1880	0.91	100%<15μ
COMPOSITION NO. 48 (.05ZnO-.335MgO-.28MnO-.335Fe_2O_3)						
28749-83V	1050	10^8	4.6	1910	0.73	100%<10μ
-90D	1100	3.0×10^7	1.9	1890	0.86	100%<10μ
-90H	1160	2.0×10^7	1.6	2020	0.87	100%<10μ
-92F	1250	2.5×10^7	1.2	1800	0.90	100%<10μ
-92K	1275	2.0×10^7	1.0	1850	0.90	100%<20μ
COMPOSITION NO. 49 (.10ZnO-.315MgO-.27MnO-.315Fe_2O_3)						
28749-92-O	1200	10^8	1.35	1270	0.70	100%<10μ
-92L	1225	2.0×10^7	1.02	1740	0.80	100%<10μ
-92R	1250	2.5×10^7	0.76	1090	0.76	100%<10μ
29271-36G	1200*	7.0×10^7	0.83	1660	0.91	100%<10μ

RCA NO. 28749-92J has $S_w = 0.52$ μsec-Oe.
All firings were for 24 hours in CO_2 except one marked * which was fired in an atmosphere of O_2.

TABLE I (Cont'd.)

FERRITE CHARACTERISTICS – PRESSED CORES

RCA NO.	FIRING Temp. (°C)	ρ (Ω-cm)	H_c (Oe)	B_m (G)	B_r/B_m	GRAIN SIZE (Microns)
COMPOSITION NO. 50 (.10ZnO-.36MgO-.18MnO-.36Fe_2O_3)						
28749-92P	1200	10^8	1.08	1640	0.88	100%<10μ
-92M	1225	8.0×10^6	0.98	1680	0.89	100%<10μ
-92S	1250	2.0×10^7	0.91	1720	0.86	100%<10μ
29271-36H	1200*	10^8	0.98	1730	0.92	100%<10μ
COMPOSITION NO. 51 (.10ZnO-.405MgO-.09MnO-.405Fe_2O_3)						
28749-92Q	1200	1.3×10^8	1.69	1760	0.82	100%<10μ
-92N	1225	1.4×10^6	1.96	1630	0.77	100%<10μ
-92T	1250	10^6	1.73	1390	0.73	100%<10μ
29271-36I	1200*	7.0×10^7	0.94	1680	0.92	100%<10μ

*These cores fired in an atmosphere of O_2. All other cores were fired for 24 hours in CO_2.

TABLE II

CHARACTERISTICS OF DOCTOR-BLADED FERRITE SAMPLES

Laminate No.	Firing Temp. (°C)	H_c (Oe)	B_m (kG)	B_r/B_m	ρ (Ω-cm)	Grain Size (microns)	T_c (°C)	$\Delta B/^\circ C$ (%)	Sw (Oe-μsec)	I_R (mA)	I_W (mA)	I_D (mA)	Aver. Signal (mV)	Back Voltage (mV/bit)
					CORE PROPERTIES					LAMINATE OPERATION				
Composition No. 19A (.03 CoO - .47 MnO - .50 Fe_2O_3)														
R-31	1170	1.40	3.0							75	40	±19	±1.5	16
CW-2	1040	0.75	2.50	0.78	2×10^4	<10μ	295	0.14	0.22/0.22	Memory arrays not fabricated				
CW-3	1120	0.71	2.46	0.80	300	<10μ	295	0.14		Memory arrays not fabricated				
CW-4	1150	0.22	2.50	0.82	285	40% <10μ 60% 300μ	295	0.14	0.40/1.57	Memory arrays not fabricated				
CW-5	1200	0.21	2.15	0.65	400	300μ	295	0.14	0.36/0.50	Memory arrays not fabricated				
Composition No. 26E (.027 CoO - .513 MnO - .46 Fe_2O_3 + 1% MgO by weight)														
28749 - 94 I	1100	0.53	2.00	0.89	8.6×10^4	85% <10μ 15% large	250	0.13	0.28/0.28	Inoperable				
- 94 G	1150	0.35	2.66	0.89	2.4×10^4	large	250	0.13	0.31/0.31	Inoperable				
- 94 B	1200				3.2×10^4	large	250	0.13		Inoperable				
Composition No. 28B (.60 MnO - .40 Fe_2O_3 + 1% MgO by weight)														
- 95 B	1100	1.85	1.43	0.87	10^6	2-7	220	0.10	0.53/0.53	100	95	±14	±0.5	14
- 99 A	1150	1.72	1.40	0.93	1.7×10^6	5-10	220	0.10	0.45/0.45	100	95	±18	±0.5	17
- 95 A	1175	1.41	1.35	0.89	2.5×10^6	3-10	220	0.10	0.44/0.44	100	90	±12	±0.5	14
- 94 A	1200				5×10^5		220	0.10		100	80	±15	±0.5	25
- 95 C	1200	0.47	1.20	0.95	1.8×10^6	7-15	220	0.10	0.48/0.48	100	95	±10	±0.5	16
- 94 H	1225	0.52	1.66	0.93	2×10^6	large	220	0.10	0.47/0.47	100	95	±10	±0.5	16
Composition No. 41 (.40 MgO - .20 MnO - .40 Fe_2O_3)														
- 97 E	1200	2.64	.85	0.58	1.2×10^8	<10μ	280	0.12	1.05/1.05	100	75	±24	±1.0	14
- 97 C	1225	1.28	1.05	0.94	1.2×10^8	<10μ	280	0.12	1.0/1.0	95	70	±15	±1.4	18
- 97 A	1250	0.95	1.32	0.91	2.4×10^8	7-50	280	0.12	1.0/1.0	85	70	±10	±1.25	23
Composition No. 47 (.05 ZnO - .19 MnO - .38 MgO - .38 Fe_2O_3)														
- 97 F	1200	1.60	1.44	0.79	3.2×10^7	<10μ	262	0.18	0.39/0.39	100	90	±12	±1.5	9
- 97 D	1225	0.76	1.01	0.95	2.2×10^7	<10μ	262	0.18	0.50/0.50	85	45	±10	±2.1	8
- 97 B	1250	0.95	1.08	0.92	7×10^8	5-50	262	0.18	0.68/0.68	90	65	±10	±1.9	27

cores. The pressed cores were evaluated as part of the materials study and the drive current was selected to produce magnetization values approaching saturation magnetization. Under this condition, meaningful data for fundamental values of the various compositions could be compared. The doctor-bladed cores were made and tested as part of the array investigation and the drive current was selected so as to delineate the "disturb sensitivity" of the core as it would function in a memory environment. If the loop, under these conditions, has a nonsquare corner, the material is disturb sensitive, and the corresponding laminate operation is degraded.

B. Coercive Force

To drive laminated ferrite arrays at low power from integrated circuits, the ferrite must have a sufficiently low coercive force. For a ferrite material, this force is a function of several parameters. The primary influence is the major crystal anisotropy constant (K_1), which varies with chemical composition. This anisotropy constant, measured in ergs/cm^3, describes the difficulty in rotating the magnetization vector from an easy to a hard direction of magnetization in a single crystal. When K_1 is small, a change in magnetization direction is accomplished with little expenditure of energy. Consequently, the coercive force is low.

K_1 for most ferrites has a negative sign; an exception is $CoFe_2O_4$ which has a very large positive value of K_1. Since a very small value of K_1 is desired to produce a small coercive force, it is often possible, by appropriate Co substitutions, to reduce the coercive force. An example of this effect may be seen by comparing the coercive force data for Compositions No. 26 and 26A as listed in Table I and plotted in Figure 2.

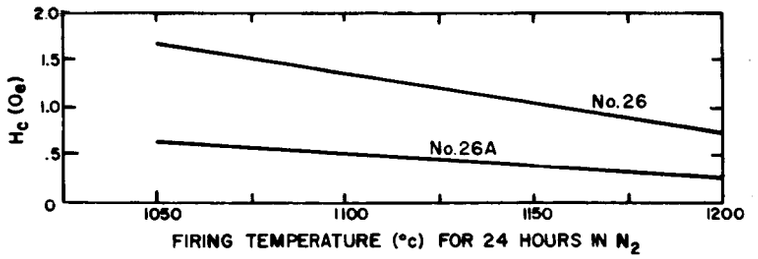

Figure 2. The influence on H_c by the substitution of Co for Mn in Mn-Fe ferrite. Composition No. 26 - (.54 MnO-.46 Fe_2O_3).Composition No. 26A - (.027 CoO-.513 MnO-.46 Fe_2O_3).

It is not possible to reduce the coercive force without limit by this means, because of the existence of the higher order anisotropy constants (K_2, K_3 ...). Since the anisotropy constants are not directly interrelated, they cannot all be made to have zero values simultaneously.

The influence of grain size on coercive force is associated with the ease of magnetization vector displacement. From domain theory,[7] it may be shown to

be energetically more favorable for magnetization to change through the mechanism of domain wall motion. This leads to a lower value of coercive force than if the magnetization had to rotate. If the grains are small enough to preclude the presence of domain walls within the grain (single-domain size grains), the magnetization direction can be changed only by rotation. Being energetically more demanding, the result is a much higher coercive force. Table I illustrates these trends, for example, Composition No. 14 and 17.

C. Switching Properties

1. Introduction. -- The memory cell in a laminated ferrite array is of micro-dimensions. To generate a readily detectable sense signal, the cell must switch rapidly. The switching time τ of a cell is determined by two quantities: the inherent "switching speed" of the ferrite material and the magnitude of the average applied field (H) are determined by the cell dimensions and the magnitude of current flowing through the cell. The application of large read and write currents can make switching very rapid; the switching time τ can then be in tens of nanoseconds.[6] Previous work with low coercive force laminates indicated that reasonable sense signal magnitudes are obtained at switching times on the order of 0.2 to 0.3 microsecond.[2] These switching times can be obtained at low drive currents if the ferrite material has sufficient "switching speed."

2. Theory. -- The switching process in polycrystalline ferrites is not completely understood.[7,8] A magnetic moment is associated with certain of the electron spins in the ferrite. In a toroid in a remanent state, these moments are aligned with one another so as to produce a net magnetic flux in, say, the clockwise direction. If a current of proper polarity is applied to a wire linking the toroid, the resulting field (H) produces a torque on these moments so as to cause the net flux to become counterclockwise. The flux reversal process is not instantaneous because a certain amount of energy is given up to the lattice during the switching, i.e., there is a "friction" of sorts. Because the ferrite is polycrystalline with crystallite axes in random directions, and because of the presence of defects such as pores, local regions or domains of reversed magnetization remain even in the remanent state. These regions are separated from the regions of "proper" direction of magnetization by domain walls; the magnetization direction rotates smoothly across the wall changing by 180°.

The flux reversal process takes place by domain wall motion if the reversing field (H) is slightly larger than the coercive force (H_c).[9] In this process, the local regions of reversed magnetization expand at the expense of unreversed regions. The reversing field causes new regions of reversed magnetization to form at crystal defects; this is called domain nucleation. These domains will also expand during the switching process. Thus, wall switching time is related to structural properties of the ferrite, because the greater the density of defects, the greater the number of walls participating in switching. The larger the number of walls, the shorter the distance they must move and consequently, the shorter the switching time. The details of domain nucleation and energy transfer during switching are not well enough understood to make any a priori predictions of wall switching behavior in polycrystalline ferrites.

Flux reversal in toroids under the influence of very high applied fields is thought to take place by a uniform rotation of the magnetic moments.[10] Some features of very-high-speed switching can be successfully explained, but again the details are not predictable.

Flux reversal caused by applied fields between these two extremes of very-high and just-above threshold, which is the region of interest in most practical memories, is not well understood. Nucleation and wall motion are undoubtedly important at fields well above the coercive force (H_c) but may not be the sole mechanism over the entire range of our measurements, which are described next.

3. Experimental Technique. -- The switching time τ is measured as a function of the mean applied field (H). The inverse switching time ($1/\tau$) is plotted as a function of (H). A typical plot is shown in Figure 3. The inverse slope of this curve, called S_w, is a measure of the switching performance of a given toroid. The lower the value of S_w the better, since a low S_w implies a steep slope which in turn indicates a large decrease in τ for a small increase in H.

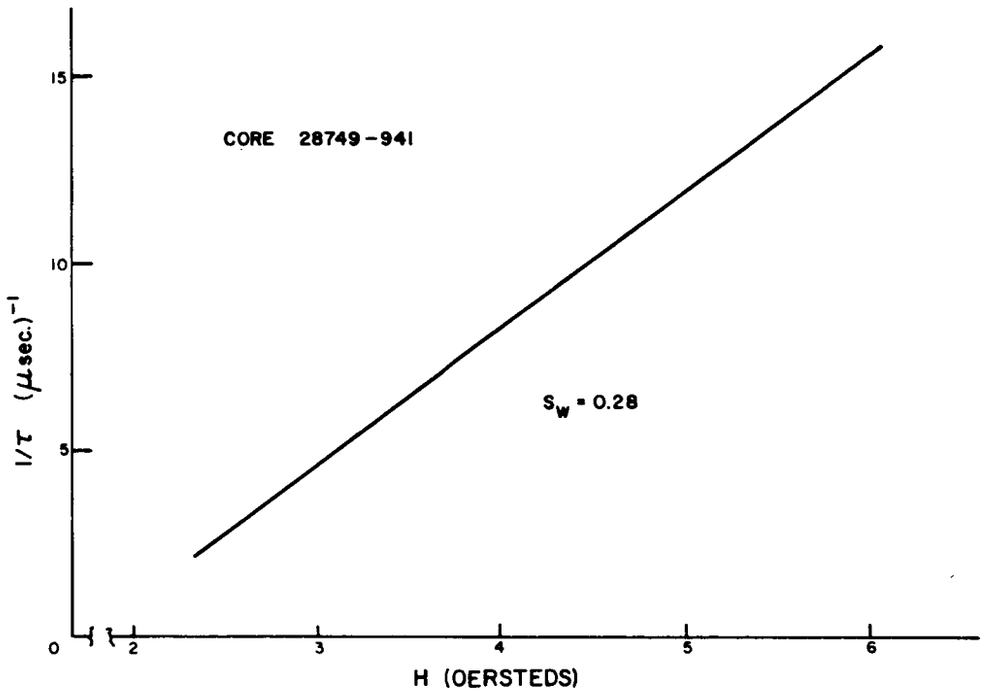

Figure 3. Inverse switching time vs. field (Core No. 28749-94I).

A typical switching waveform, the voltage induced in a winding linking the test toroid, is shown in Figure 4. The applied reversing current has a risetime of approximately 5 nsec, and the two sharp spikes at the leading and trailing edges of the waveform are induced voltages caused by the linear inductance of the core. The switching time τ is defined here as the time from the initiation of switching to the time that the signal drops to 10% of its peak value, as indicated in Figure 4.

The experimental setup is sketched in Figure 5. The fast-rising reversing or reset current is generated by discharging a cable with a free-running mercury relay. The width of the reset pulse is determined by the cable length and is slightly less than 0.5 μsec for these experiments. Thus, all measured values of τ are 0.5 μsec or less, which is the area of interest for laminated arrays. The amplitude of the reset pulse can be varied over the range 0 to 4 amperes. The corresponding variation in H is a function of the core radius and the number of turns. Each reset pulse is followed by a 20 μsec setting pulse which establishes a consistent remanent state. The amplitude of the set pulse is adjusted to three times the minimum amplitude required to fully switch the toroid.

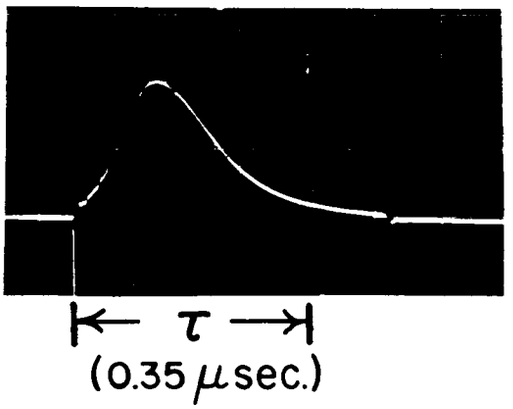

Figure 4. Toroid switching waveform.

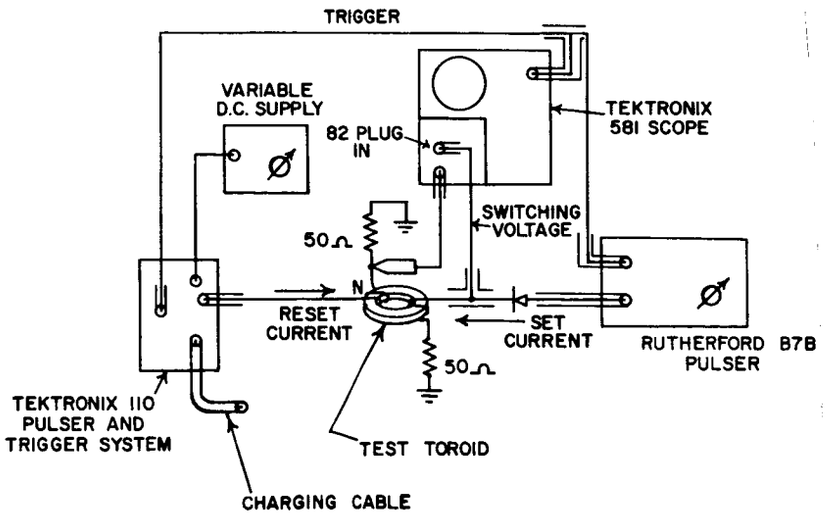

Figure 5. Experimental arrangement for measuring switching speed.

Both pressed cores and "doctor-bladed" cores have been tested. S_w was not measured for all the experimental cores because a reasonable hysteresis squareness is necessary for the measurement to have validity. Cores with poor squareness appear faster than they are because their large elastic flux (reversible flux) follows the risetime of the reversing field. Other cores were not measured because of inappropriate values of other parameters.

4. Experimental Results. -- A typical switching curve, from which the switching coefficient (S_w) is calculated, is shown in Figure 3. Note that the inverse switching time ($1/\tau$) varies linearly with H over the entire range studied (approximately 2 to 6 Oe). In general, the switching curve is not linear over a range encompassing switching times from several microseconds down to several nanoseconds; in fact, the full curve may be more parabolic than linear. For this reason some of the measured experimental cores yield switching curves, typified by Figure 6, with two "linear" regions. The region at higher drive field has a steeper slope, and consequently a lower S_w, than the region at lower drive field. This may be due to rotational mechanisms beginning to contribute to switching at higher fields. Thus, the S_w data in Tables I and II are presented in the form:

S_w at higher drive/S_w at lower drive.

If the curve is linear over the range, the two values are equal.

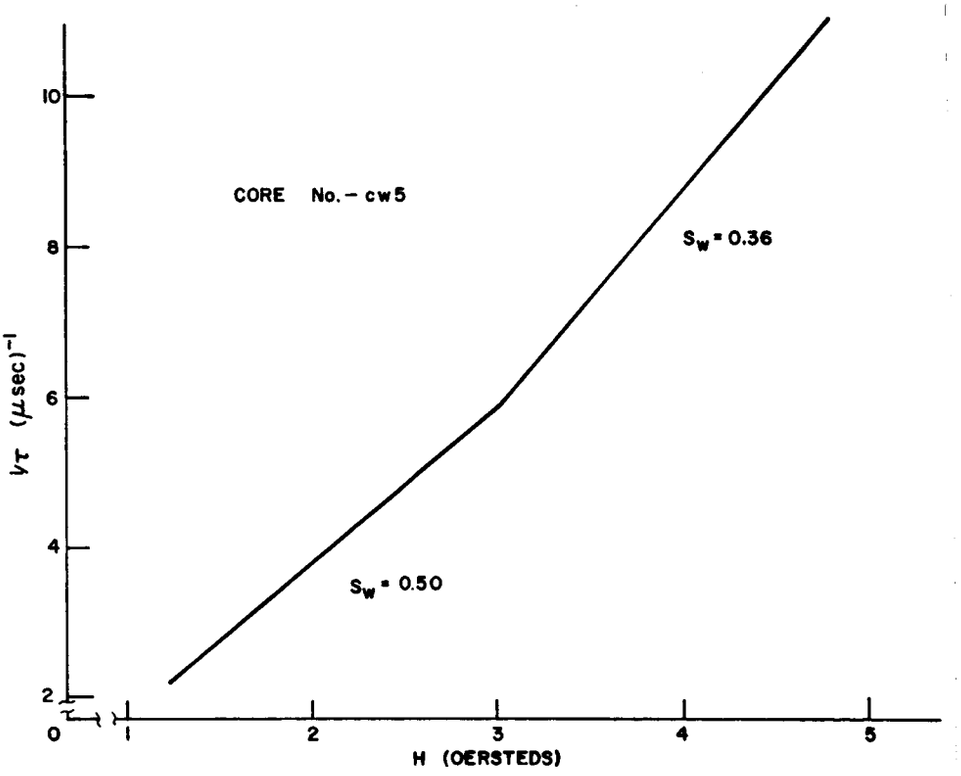

Figure 6. Inverse switching time vs. field (Core No. CW5).

The existence of nonlinearity in the switching curve, makes a detailed comparison between various materials somewhat difficult. All the studied materials with grain size in the region of 10 μ or less, with the exception of Composition No. 41, have a high drive S_w of 0.5 or less. The switching waveforms for Composition No. 41 are characterized by a long tail of significant amplitude whose duration is not very sensitive to drive field, and it has a correspondingly high S_w. (This deficiency is confirmed by the data on laminate operation reported later in Section V.) The switching waveforms of Composition No. 47 do not have a long "tail"; consequently, the measured S_w's are considerably lower and decrease with decreasing grain size, as would be expected.

D. Grain Size

From practical as well as operational considerations, polycrystalline materials must be used for the laminated ferrite memory. The concern with grain size in the laminate originates from the need to restrict the grain size to much less than the memory cell size. If the grains are allowed to grow in an unrestricted way, nonuniform operation of the memory would result.[11] Since the spacing between the orthogonal conductor planes is 13 microns (0.0005 inch), the grain size should be limited to 10 μ or less.

The grain size and distribution are obtained by petrographic observation. The samples are highly polished and etched. Etching in an acid solution removes a small amount of the polished surface in a preferential manner. Consequently, the grains, grain boundaries, and imperfections are visible to microscopic observation.

The grain size is influenced primarily by the firing conditions. For all compositions, the grain size increases as the firing temperature is increased. Referring to Figure 7, we see that for Composition No. 28 the grains start to grow only after a firing temperature of 1150°C is reached. In contract, Composition No. 17 exhibits spontaneous grain growth when the firing temperature exceeds 1035°C due to the presence of lithium ions.

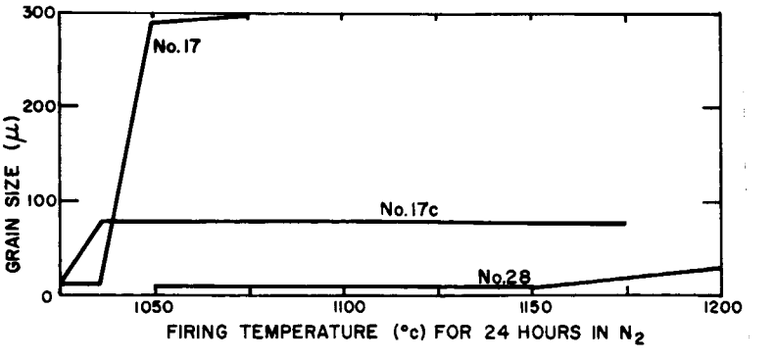

Figure 7. The grain size of some ferrites as a function of firing temperature. Composition No. 17 - (.03 LiF-.54 MnO-.52 Fe_2O_3). Composition No. 17C - (.03 LiF-.54 MnO-.52 Fe_2O_3) + 0.25 wt. % SiO_2. Composition No. 28 - (.60 MnO-.40 Fe_2O_3).

For Composition No. 17, the grain size is of the order of 10 μ for firing temperatures below 1035°C. The coercive force greatly exceeds 1 Oe, and this may not be used for the memory. For firing temperatures above 1050°C, the coercive force drops to an acceptable value; however, the grain size is far too large for laminated arrays. For the intermediate region (1035°C to 1050°C) control of grain size is not feasible. This general behavior is characteristic of all the lithium bearing ferrite compositions investigated. On the basis of these data we decided to investigate other compositions.

Certain compositional modifications can limit the grain size. This effect is shown in Figure 7 in the case of Composition No. 17C. In this case 0.25 wt.% of SiO_2 was added to Composition No. 17. The grains grew to a limiting size of about 80 μ.

E. Squareness

The shape of the hysteresis characteristic of the ferrites is determined by anisotropy. Three types of anisotropy can be important in this consideration, namely shape, stress, and crystal. In the configurations used for most ferrite memories, shape anisotropy has no effect because of the closed magnetic path. Stress anisotropy is manifest if the ferrite has appreciable magnetostriction.

The squareness observed in the ferrites of this project is a result of the crystal anisotropy and magnetostriction interacting in the appropriate crystallographic direction. In most cubic ferrites the easy direction of magnetization is the crystallographic [111] direction. If the magnetostriction constant in the [111] direction (λ_{111}) is small, the hysteresis loop will be rectangular. The magnetization vector adheres to the [111] direction with a force proportional to the anisotropy constant K_1. Further, if λ_{111} is negligible, random stresses cannot influence the magnetization vector. The magnetization vector thus remains bound in the [111] direction until the applied field is of a magnitude to reverse the direction of magnetization, and the ferrite has a square loop characteristic. If λ_{111} were not negligible, stresses acting by way of magnetostriction would alter the coupling between the magnetization vector and the [111] direction. The result is a nonsquare loop.

Table I shows the composition and squareness value for all the ferrites produced during the contract. In general, a good squareness ratio (B_r/B_m) is observed. However, as can be seen, the squareness varies primarily with composition. The magnetostriction constant was not measured, but it seems certain that in some compositions the value of λ_{111} is not negligible. A good case in point is Composition No. 19 with a squareness above 0.90. When Co ions are incorporated (Composition No. 19A) the squareness decreased appreciably. While the crystal anisotropy K_1 is reduced, as shown by the decrease in coercive force, the new value of λ_{111} is increased.[12]

F. Thermal Characteristics

As discussed under the heading of Magnetic Induction (IV-A), the ferrites have A sites and B sites. There is an energy (exchange energy) which maintains the spin alignment configuration of these two sites. The A site moments can be considered to point in one direction and the B site moments point in the opposite direction. This arrangement results in a net moment or magnetization.

Thermal energy, on the other hand, endeavors to produce a random orientation of the spin moments. Since the thermal energy is a function of temperature, the alignment of the moments (magnetization) is a function of temperature. As the temperature is increased, the exchange energy tends to be overcome and the net moment or magnetization is reduced. At the Curie Temperature the thermal energy dominates and the material is no longer ferrimagnetic.

Considering the different site moments for various ferrites, it is not surprising that B vs. T characteristic is not the same for all ferrites. When the normal ferrite Zn Fe_2O_4 is substituted in an inverse ferrite, the Curie temperature is reduced because of the weakened interaction between the A and B sites.

Table III shows the major compositions that were synthesized during the contract, their Curie temperature, and the change of magnetization as the ambient temperature is varied from 25°C to 125°C. The measurement of the Curie temperature and the change of magnetization as a function of ambient temperature employs the principle of measuring the force exerted on a sample by an inhomogeneous dc field as the sample temperature is changed.[13]

Small substitutions or additions of CoO, SiO_2, CuO, MgO, Al_2O_3, Bi_2O_3, or glass were used to alter some of the properties of the basic compounds. The substitutions and additions, being of small amount, have only a minor effect on the shape of the B vs. T curve and the Curie temperature.

Figure 8 shows the complete magnetization-temperature characteristic of Compositions No. 41 and 47. These compositions are among those used to fabricate laminated memory arrays. For comparison, the figure also shows the characteristic of the ferrite used in Phase I of the project. While the Curie temperature goal of 300°C was not quite achieved in these materials, the thermal stability of magnetization over the temperature range of interest is greatly improved (about threefold).

Figure 9 shows the change of coercive force, under constant drive conditions, as a function of ambient temperature for Compositions No. 41 and 47. These data were taken from hysteresis loops (400 cycles) at various temperatures. For the compositions shown, the coercive force changes about $\pm$ 10% from 0°C to 50°C.

TABLE III
THE THERMAL CHARACTERISTICS OF FERRITE COMPOSITIONS

COMP. NO.	MOLAR COMPOSITION					T_c (°C)	% ΔB/°C
	LiF	MnO	Fe_2O_3	ZnO	MgO		
14	.09	.50	.41			235	.19
15	.07	.48	.45			283	.15
16	.03	.48	.49			290	.16
17	.03	.45	.49			306	.09
18	.05	.41	.54			330	.11
19		.50	.50			295	.14
20	.01	.52	.47			273	.16
21	.03	.50	.47			284	.22
22	.01	.48	.51			283	.15
23	.01	.49	.50			278	.14
24	.01	.50	.49			276	.18
25	.01	.51	.48			273	.15
26		.54	.46			250	.13
27		.57	.43			240	.17
28		.60	.40			220	.10
29		.51	.44	.05		221	.19
30		.55	.40	.05		217	.21
31		.57	.38	.05		210	.20
35		.49	.46	.05		223	.12
36		.44	.46	.10		205	.12
37		.39	.46	.15		160	.13
38		.44	.46		.10	292	.08
39		.34	.46		.20	315	.14
40		.24	.46		.30	330	.10
41		.20	.40		.40	280	.12
42		.28	.36		.36	254	.20
43		.39	.46	.05	.10	250	.20
44		.29	.46	.05	.20	270	.19
45		.19	.46	.05	.30	292	.17
46		.19	.46	.10	.25	250	.22
47		.19	.38	.05	.38	262	.18
48		.28	.335	.05	.335	240	.24
49		.27	.315	.10	.315	165	.42
50		.18	.36	.10	.36	190	.38
51		.09	.405	.10	.405	178	.36

% ΔB/°C is the value over the temperature range of 25 to 125°C.

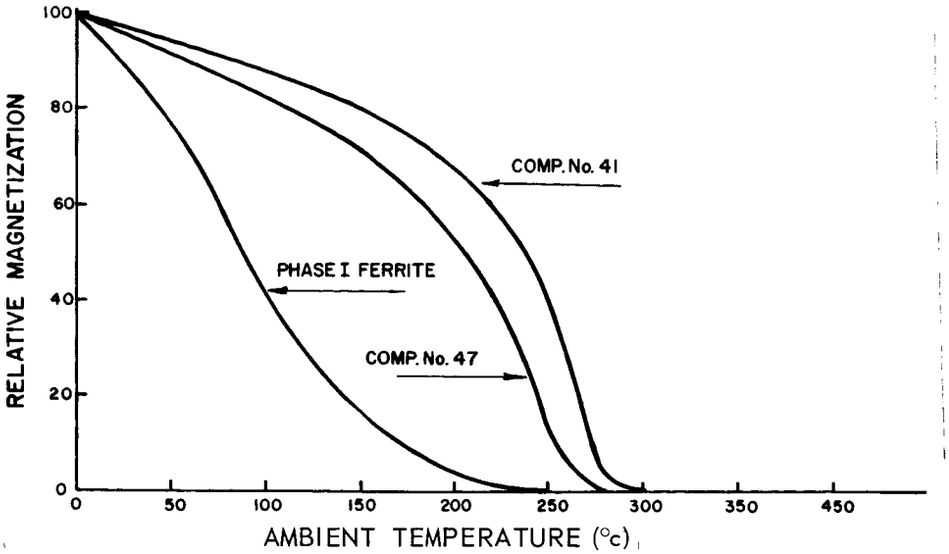

Figure 8. Relative magnetization as a function of ambient temperature for several ferrites of interest to this project.

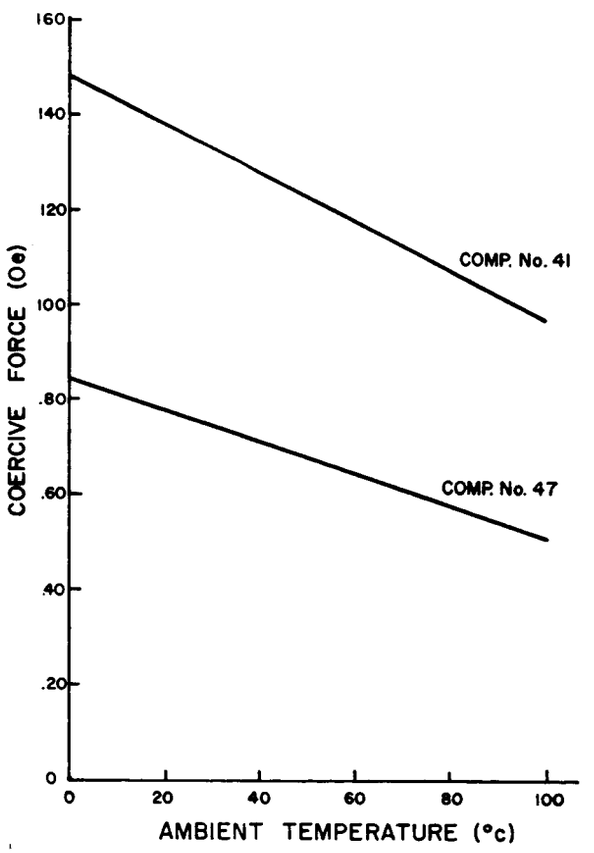

Figure 9. The change of coercive force as a function of ambient temperature for a sample of compositions No. 41 and No. 47.

G. Resistivity

Ferrites with identical elements in more than one valence state on equivalent crystallographic lattice sites generally have low resistivity. The resistivity of these ferrites is very sensitive to the relative amounts of such ions. For example, the resistivity of Fe_3O_4 is about 10^{-3} Ω-cm. The iron is present as Fe^{++} and Fe^{+++} ions located on octahedral sites. Conduction takes place by the energetically easy movement of electrons between Fe ions. $NiFe_2O_4$ has a resistivity of 10^6 Ω-cm. To obtain this high resistivity it is necessary to avoid the formation of Fe^{++} ions by using an oxidizing atmosphere during the firing. Also, an excessive firing temperature must be avoided because iron oxide tends to lose oxygen at high temperatures and thus, to maintain electrical neutrality, Fe^{++} is formed. To obtain good square-loop properties from $MnFe_2O_4$ a protective atmosphere (CO_2) must be used. Under these conditions a few Fe^{++} ions form, thus accounting for the observed resistivity.

Tolksdorf[14] reports that the resistance of a hexagonal ferrite may be increased by several orders of magnitude, by adding Bi_2O_3 to this ferrite. For this reason, Composition No. 26 (.54 $MnCO_3$-.46 Fe_2O_3) was modified to have 0.005, 0.01, and 0.03 moles of Bi_2O_3 substituted for Fe_2O_3. It was found that the resistivity is increased slightly. The substitution of Bi_2O_3 for Fe_2O_3 (in Tolksdorf's case) results simply in an iron-deficient sample, having started with a stoichiometric material. Since Composition No. 26 is already iron-deficient, the change in resistivity brought about by a further small decrease in iron content is small.

The high resistivity observed in the preferred compositions (Nos. 41 and 47) of this project is the result of all the Mn and Fe ions being in the trivalent state, since no divalent Mn or Fe ions are needed for stoichiometry. Table I shows the composition and resistivity values for all the compounds made under the contract.

H. Discussion

The various ferrite characteristics are discussed above as individual materials properties. A theoretical basis for these properties is related to the experimental results obtained. Of course, there is great interdependence between some of the characteristics. Unfortunately, it is not possible to optimize all of the properties in a given sample.

The greatest interdependence is between grain size, coercive force, and switching coefficient. In general, the lowest value of coercive force for a ferrite is obtained if it is in the form of a single crystal with a closed flux path, such as a "window frame". However, the ferrite switches most slowly under these conditions.[15] On the other hand, the highest coercive force and the fastest switching is found when the ferrite is composed of single-domain grains (submicron size). The materials described have grain sizes between these two extremes, with the result that the materials with the smallest grains have higher values of coercive force and lower switching coefficient (faster switching).

The resistivity goal of 10^6 Ω-cm is difficult to attain while retaining the other requirements. For example, Composition No. 19A essentially fulfills the goals except for the resistivity requirement. To circumvent the resistivity difficulty, a few experiments were performed with an insulating sheet incorporated in the laminate. The construction was essentially the same as the usual laminated array except that a very thin (0.0003-in.) doctor-bladed sheet of MgO is placed between the two sets of conductors. Although the sample had increased resistivity (about tenfold), it was still too low for satisfactory operation. Polished sections of this sintered laminate indicated that the MgO layer is not continuous. A slightly thicker insulating layer may be better but the closed flux path could be seriously affected as a result.

The best compromise is Composition No. 47. Data from doctor-bladed toroids of this composition are compared with the project goals in Table IV.

TABLE IV

COMPARISON OF FERRITE PARAMETERS

Parameter	Goal	Best Effort
Coercive force (Oe)	≤ 0.5	0.76
Remanent flux density (G)	≥ 1000	1010
Squareness ratio (B_r/B_m)	≥ 0.9	0.95
Resistivity (Ω-cm)	$\geq 10^6$	2×10^7
Curie temperature (°C)	≥ 300	262
Switching coefficient (μsec-Oe)	≤ 0.5	0.50

The "best effort" cores are fired with laminate No. 28749-97D (see Table II) and have small grain structure. These data are obtained from toroids cut from doctor-bladed sheets of Composition No. 47. In addition, laminated memory arrays were fabricated and sintered with these "best effort" cores. The data for these "best effort" cores and laminated arrays are given in Table II for laminate No. 28749-97D. Both the "best effort" cores and the laminates are fine grained.

In Table I it is seen that the measured magnetic and electrical properties of pressed cores made from Composition No. 47 are different from the characteristics of doctor-bladed cores. The reason for this difference is explained in Section IV-A.

V. LAMINATED FERRITE MEMORY ARRAYS

A. Introduction

Five of the experimental compositions were utilized to fabricate laminated ferrite arrays, namely Compositions No. 19A, 26E, 28B, 41, and 47. Section III gives the fabrication procedure.

Composition No. 19A was selected to determine the effect of variation in grain size on laminate operation. Some of the earlier compositions achieved the coercive force goal of the program only if grains of large size, up to 300 μ, could be utilized. The spacing between conductors in a laminate is on the order of 13 μ; thus, large grains could encompass one or more storage locations. Since the crystallographic orientation of these grains with respect to the conductor orientation and the location of grain boundaries cannot be controlled, nonuniform magnetic behavior would be expected. To test this hypothesis, Composition No. 19A was used to fabricate an array.

Compositions No. 26E and 28B were chosen as the best materials having compositions near $MnFe_2O_4$. Compositions No. 41 and 47 incorporated significant quantities of Mg so as to yield much higher resistivity than Compositions No. 26E and 28B.

To summarize, it has not been possible to optimize all of the desired properties in a single fine-grain ferrite. It is found that fine grains are necessary to achieve uniform outputs. A variety of compositions were selected for array fabrication to determine which compromise of ferrite properties would result in array characteristics compatible with the system requirements.

B. Experimental Techniques

The fabricated 256 x 100-conductor arrays with conductors (on 10-mil centers) are abraded along all four edges to expose the conductors. For array testing, one end of the 100 longer lines (digit lines) are connected in common to ground. The 256 shorter lines (word lines) are also grounded, as they would be in a system driven by MOS switches. The arrays are mounted on copper-glass epoxy boards which have linear patterns of isolated pads on 50-mil centers along the edges. This permits as many as 32 of the 100 digit lines and 64 of the 256 word lines to be accessed using the pads. A hand-soldered 2-mil silver wire serves as the connection between pad and array. Readily moveable mechanical connections interconnect the selected pad to cabling attached to the electronic pulsers and sensors. The experimental setup is sketched in Figure 10.

The laminated ferrite array is word-organized (linear select), i.e., the word lines carry full read and write currents and the digit lines carry digit currents and the sense signals. The array is operable in a one-crossover-per-bit mode at low power levels. To store a binary "0" in a cell, a positive digit current is applied in time coincidence with the write current, and negative digit current is applied to store a binary "1". Thus a stored "1" can be disturbed by positive digits and vice versa. A "worst case" test program

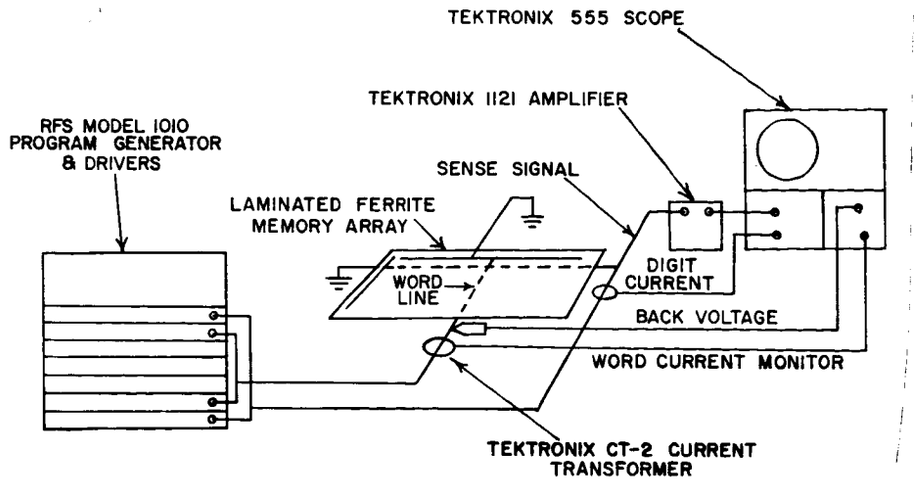

Figure 10. Experimental arrangement for measuring array operation.

is shown in Figure 11; the program incorporates the digit disturbs in combination with "pre-write" pulses which tend to minimize the stored flux because of history. The pre-write effect, for example, causes a "1" written in a cell after a read-write of a "0" to be slightly weaker upon reading than a "1" written after a read-write of a "1".

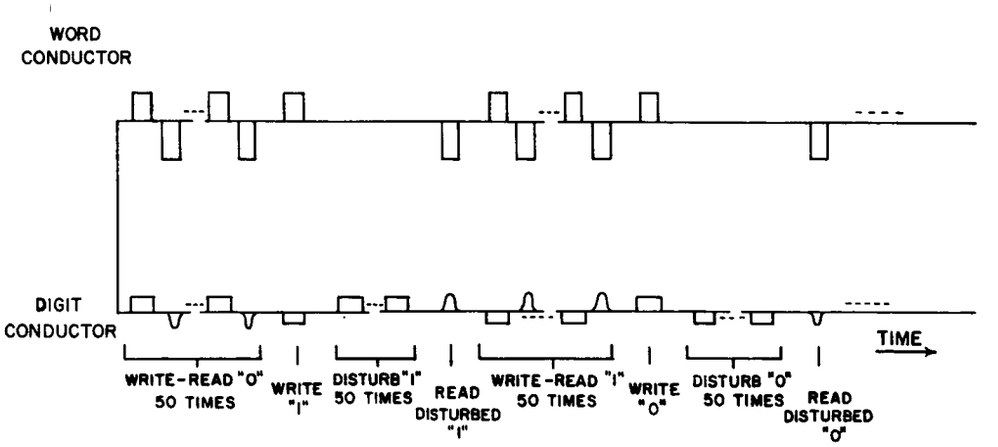

Figure 11. Memory test pulse program.

The experimental operating data to follow is divided into two parts: First, preliminary data which cover laminates made of a variety of compositions sintered under various conditions, in laminated array form, and second, a section covering the operation of the arrays with the best overall system characteristics.

C. Preliminary Data

The preliminary data on laminate operation are summarized in Table II. The test data on sample R-31 (a 256 x 100-conductor array of Composition No. 19A) are repeated from an earlier report.[11] Although the average signal obtained from this sample, 1.5 mV at 75-mA read current, is sufficiently high, there is an unacceptable lack of signal uniformity as seen in the histogram of Figure 12. This nonuniformity is due to a lack of physical homogeneity of the sample, i.e., the presence of large grains encompassing either entire memory cells or large fractions of a cell volume. These large grains are clearly visible in the cross section of Figure 13. The results obtained from array R-31 confirm the supposition that grain growth must be controlled to obtain uniform outputs from memory arrays.

The sluggishness of switching in the samples of Composition No. 26E make them totally inoperable at drive currents on the order of 100 mA, and, in fact, to obtain signals on the order of 1 mV, a read current of nearly 400 mA is necessary. The explanation for the sluggishness is that the word lines adjacent to the one selected are not sufficiently isolated due to the low ferrite resistivity and act in a fashion similar to a shorted turn on a transformer, inhibiting flux switching.

The samples fabricated with Composition No. 28B are superior in operation to those of Composition No. 26E because of their higher resistivity. However, their performance in terms of signal amplitude is inadequate for reliable system operation. This low amplitude is due to both slow switching and disturb sensitivity. The hysteresis loops for this material have a softness of corner usually associated with disturb sensitivity. See Figure 14 for an example. This softness can occur even though the B_r/B_m ratio is high, as in the case of Composition No. 28B at most firing temperatures.

The laminate series composed of Composition No. 41 served to confirm the need for fast switching properties. Our target for S_w is 0.5 Oe-μsec or less; however, the bladed cores have values close to 1.0 at all three sintering temperatures (Table II). As a result, the switching times of the sense signal are long, and the signal amplitude is consequently lower than it should be. Switching is also slowed by the relatively high coercive force.

Samples of Composition No. 47 prepared at 1225°C firing temperature had the best combination of properties to achieve the desired system performance. Their Curie temperature is sufficiently high to permit operation over a temperature range of 0°C to 50°C with all currents held constant, as shown in Figure 15. The laminate operational data of Table II were taken on half planes (128 x 100 conductors) so as to determine optimum sintering conditions without expending the small number of fabricated samples available. Additional 256 x 100-conductor planes of Composition No. 47 have been prepared and more extensive data on their operation are given in the next subsection.

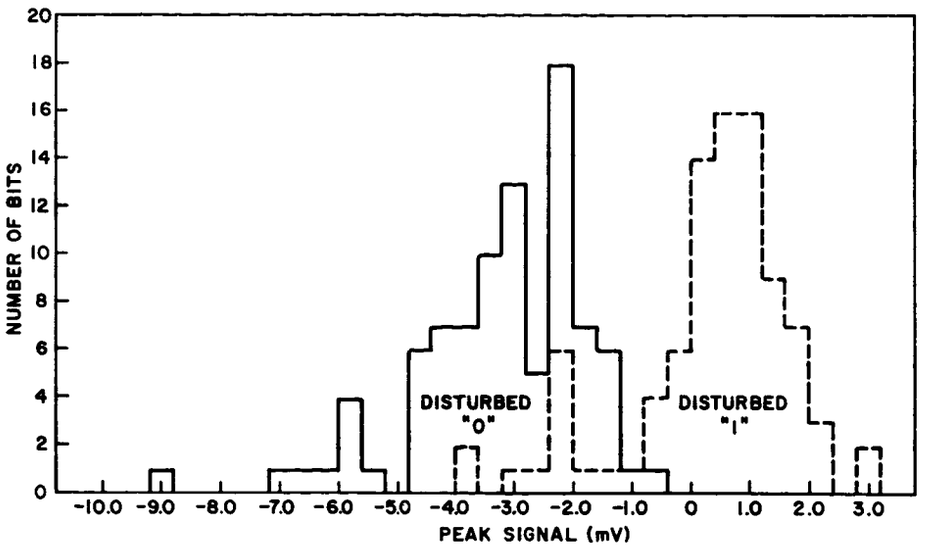

Figure 12. Histogram of output for laminate samples R-31.

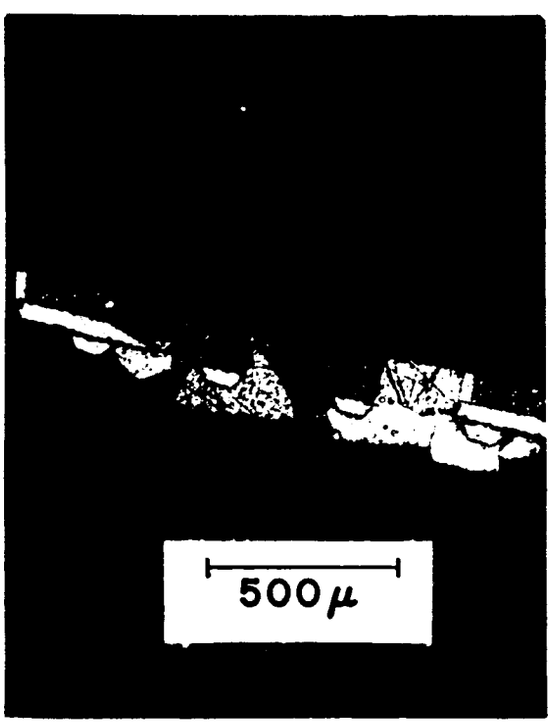

Figure 13.
Petrographic cross-sectional
view of sample R-31.

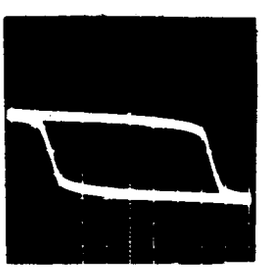

Figure 14.
Hysteresis loop - Core
No. 28749-95A.

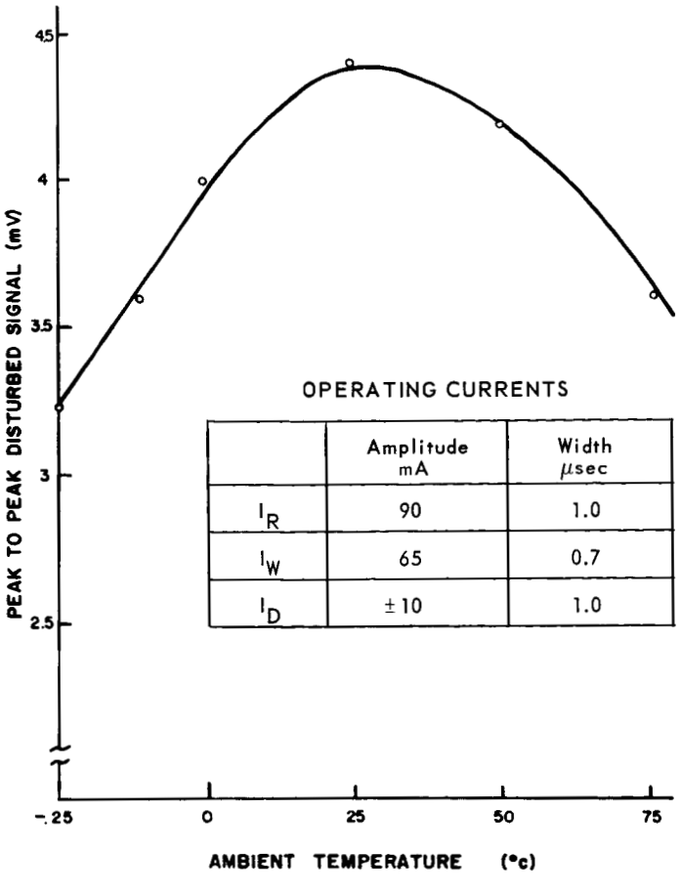

Figure 15. Signal output vs. temperature. Typical bit in Laminate No. 28749-97B. Switching time - 0.35 μsec.

D. Operating Arrays

Two 256 x 100-conductor laminated ferrite arrays have been fabricated using Composition No. 47 fired at 1225°C. One of these arrays, Number 29271-37-A, was tested to determine array operating characteristics and uniformity of output signal at room temperature. The other array, Number 29271-42-A, was tested to determine the temperature stability of operation over the temperature range 0°C to 50°C. The room-temperature behavior of the two planes is substantially identical as can be seen in the data to follow. In both cases, the read-disturb - write-disturb pulse program shown in Figure 11 is utilized. (The operating characteristics would have been improved if the disturbs had been removed from the test program.)

In the room-temperature test, the current drive pulse characteristics are:

TABLE V

LAMINATE DRIVE CURRENT PARAMETERS

	Amplitude (mA)	Width at 50% Pts. (μsec)	Rise and Fall Time (μsec)
I_R (Read)	100	0.6	0.30
I_W (Write)	70	0.5	0.20
I_D (Digit)	±18	0.7	0.25

Under these conditions, the peak back voltage developed on the word line is 9.5 mV per bit for an average peak signal of slightly less than ± 3 mV, which is 0.25 μsec wide at the base. The uniformity of signals in plane 2927-37-A is excellent, as is evident in the histogram of outputs in Figure 16. These data are for every eighth word line (32) and every seventh digit line (14) for a total of 448 tested bits. The peak signal levels are read from an oscilloscope to an accuracy of ± 0.25 mV. Thus, the histogram is actually the superposition of bars 0.4 mV wide at the base. The array is operable at read currents as low as 65 mA, but a diminution of sense signal at the rate of 0.5 mV per 10 mA is suffered as the read current is decreased from 100 mA.

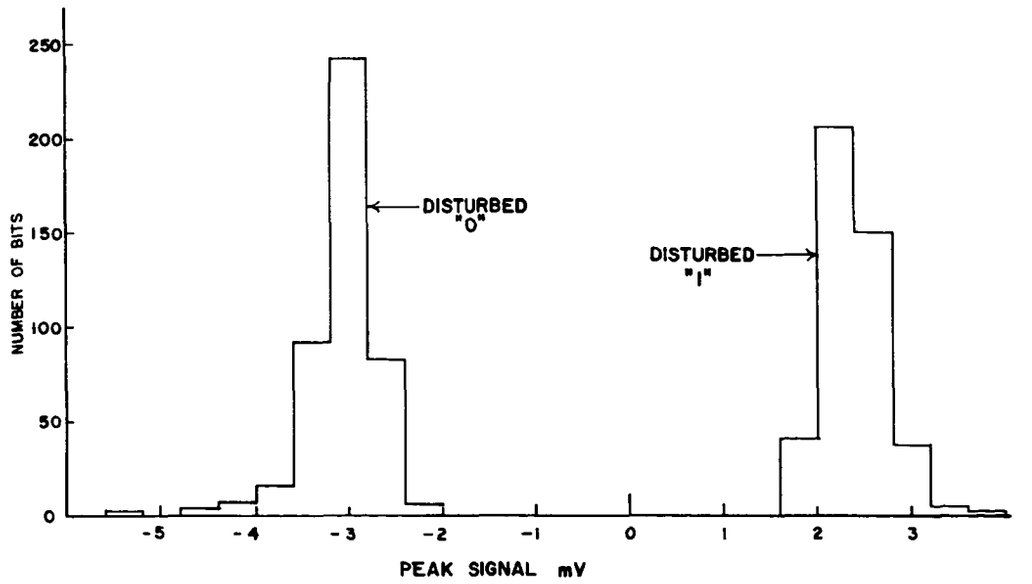

Figure 16. Histogram for 448 scattered bits. Laminate No. 29271-37A. Switching time - 0.25 μsec.

Sixteen scattered bits in array 29271-42-A were tested at 10°C intervals in the temperature range 0°C to 50°C. The drive current amplitudes for the entire temperature range are:

$$I_R = 98 \text{ mA}$$

$$I_W = 60 \text{ mA}$$

$$I_D = \pm 16 \text{ mA}$$

with the pulse widths and risetimes as shown in Table V. The write and digit currents are lower than those for the room-temperature test because they are optimal for operation at 50°C. The variation of average, minimum, and maximum "1" and "0" signals with ambient temperature is shown in Figure 17. The sense signals are 0.2 μsec wide at the base. All the tested bits remain operable over the entire temperature range. The temperature stability of this array is vastly improved compared with the arrays of Phase I. Note that the overall signals at room temperature are slightly lower than for plane 29271-37A because the currents used here are optimized at 50°C. Higher digit and write currents at room temperature results in larger signals.

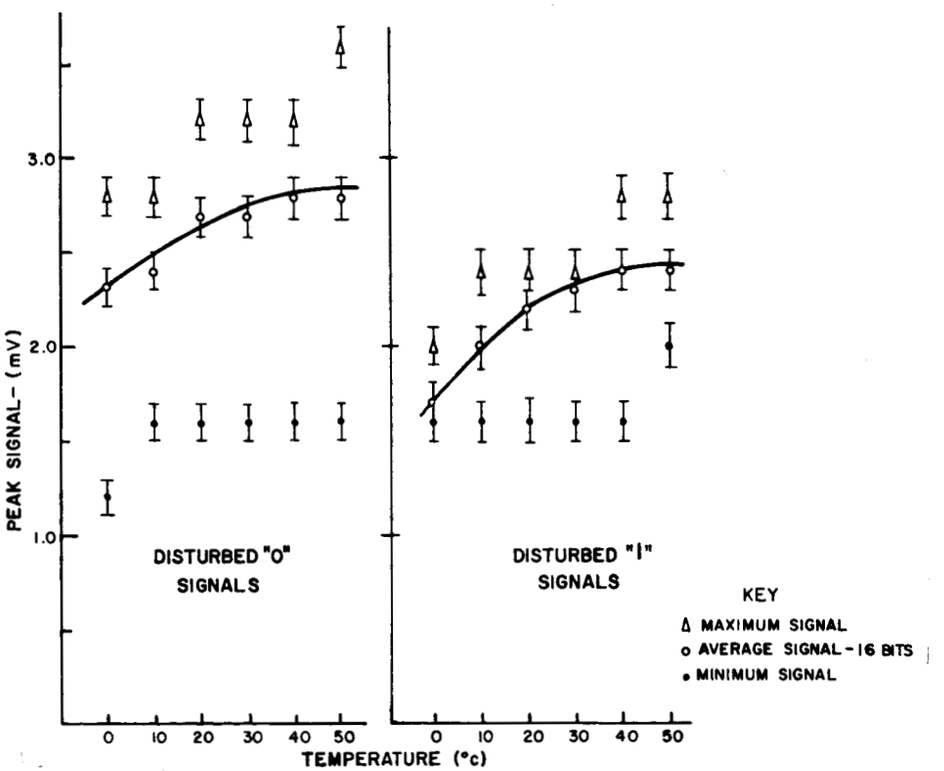

Figure 17. Signal vs. ambient temperature. Laminate No. 29271-42A. Switching time - 0.2 μsec.

In conclusion, the performance of the 256 x 100-conductor arrays fabricated from Composition No. 47 is excellent with respect to both uniformity and temperature stability. Furthermore, the arrays have operating requirements that are compatible with integrated circuits in general, and MOS integrated circuits in particular.

VI. CONCLUSIONS AND RECOMMENDATIONS

On the basis of results presented in the previous sections, the following conclusions are presented:

(1) The materials goals of the project, for the most part, have been achieved. As compared with the ferrite used in Phase I, the new materials under the present contract (Phase II) have greatly improved thermal properties. In addition, the best materials of the present investigation have high resistivity, small grains, and good squareness; however, their Curie temperature and coercive force values do not quite fulfill the goal requirements.

(2) The systems goals of the project have been achieved. An operable memory array of 256 x 100 crossovers has been fabricated and tested. This memory array has excellent operation over the ambient temperature range of 0°C to 50°C without thermal or current compensation. The output signals are high and uniform, and the back voltage is low enough to permit long words to be driven by an MOS switch.

(3) The present investigation has achieved an optimum ferrite for the specified goals, and a dramatic further gain in characteristic values seems unlikely. This conclusion is based on a thorough investigation of the ferrite systems most likely to yield the desired characteristics. However, moderate improvements in some of the parameters, such as squareness, coercive force, and switching speed could result in a substantially better systems performance.

A recommendation for future work, as a result of the present research, is to investigate some of these materials in more detail. A few compositions, such as No. 28B, 41, and 47 should be produced in pilot plant quantities to obtain improved processing quality. The influence of variations of the processing parameters, including mixing, grinding, and the final firing conditions should be investigated. Such an investigation could result in both a lower coercive force and a lower switching coefficient.

REFERENCES

1. R. Shahbender, C. P. Wentworth, K. Li, S. Hotchkiss, and J. A. Rajchman, "Laminated Ferrite Memory," Proc. Fall Joint Computer Conference, November 1963, p. 77.
2. Laminated Ferrite Memory - Phase I, NASA CR-398, March 1966.
3. R. L. Harvey, I. J. Hegyi, and H. W. Leverenz, "Ferromagnetic Spinels for Radio Frequencies," RCA Review 11, 321 (1950).
4. J. M. Hastings and L. M. Corliss, "Neutron Diffraction Studies of Mn Ferrites," Phys. Rev. 86, 1952.
5. J. Smit and H. P. J. Wijn, Ferrites (John Wiley and Sons, New York, 1959).
6. I. Abeyta, M. M. Kaufman, and P. Lawrence, "Monolithic Ferrite Memories," Proc. Fall Joint Computer Conf., 1965, p. 995.
7. H. Rubinstein, "Switching Properties of Ferrites and Garnets," Scientific Report No. 6 (Series 2), Contract AF19(604)-5487, AFCRL-62-954, November 1962.
8. G. Rado and H. Suhl, eds., Magnetism - Volume III (Academic Press, New York, 1963), p. 525.
9. Ibid., p. 538.
10. Ibid., p. 546.
11. Laminated Ferrite Memory - Phase II, Quarterly Technical Report No. 5, Contract No. NASw-979, September 1, 1965 to November 30, 1965.
12. J. Smit and H. P. J. Wijn, Ferrites (John Wiley and Sons, New York, 1959), p. 169.
13. R. L. Harvey, "Simple Force Magnetometer," Rev. Sci. Instr. 36, 1149 (1965).
14. Wolfgang Tolksdorf, "On the Preparation of Polycrystalline $Zn_2Ba_2Fe_{12}O_{22}$ Especially with Respect to the Influence of Bi_2O_3," International Conference on Magnetism, Stuttgart, Germany, 1966.
15. J. C. Miller, "Switching Properties of a Single-Crystal Specimen of Nickel Ferrite," J. Appl. Phys. 348, April 1963.

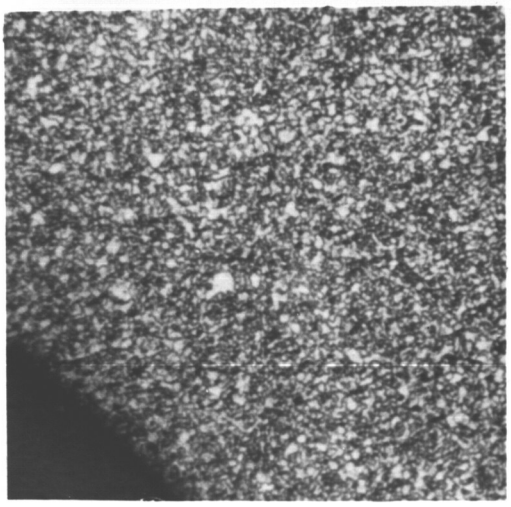

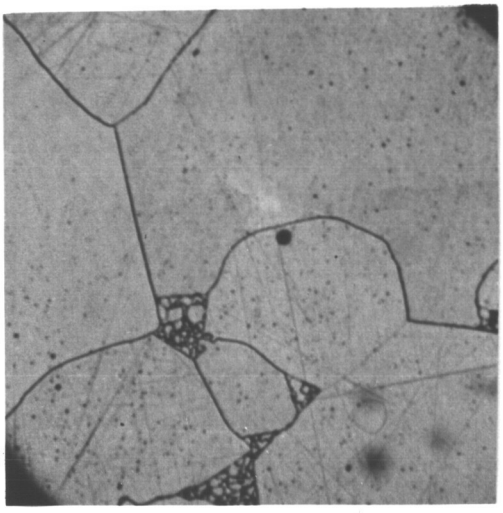

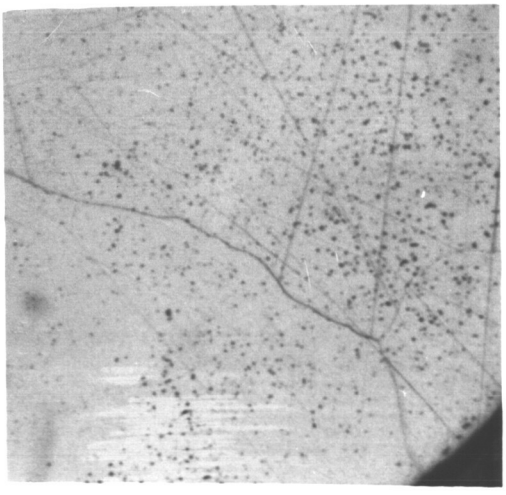

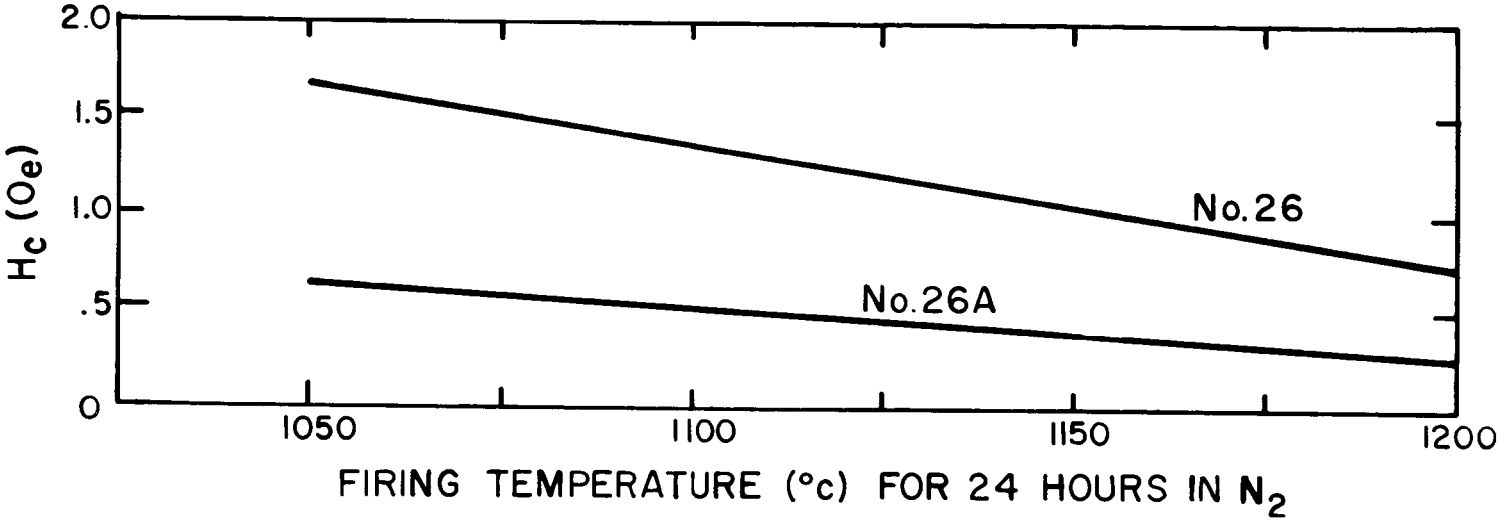
2.0
1.5
1.0
.5
0
H_c (Oe)
No.26
No.26A
1050
1100
1150
1200
FIRING TEMPERATURE (°c) FOR 24 HOURS IN N_2

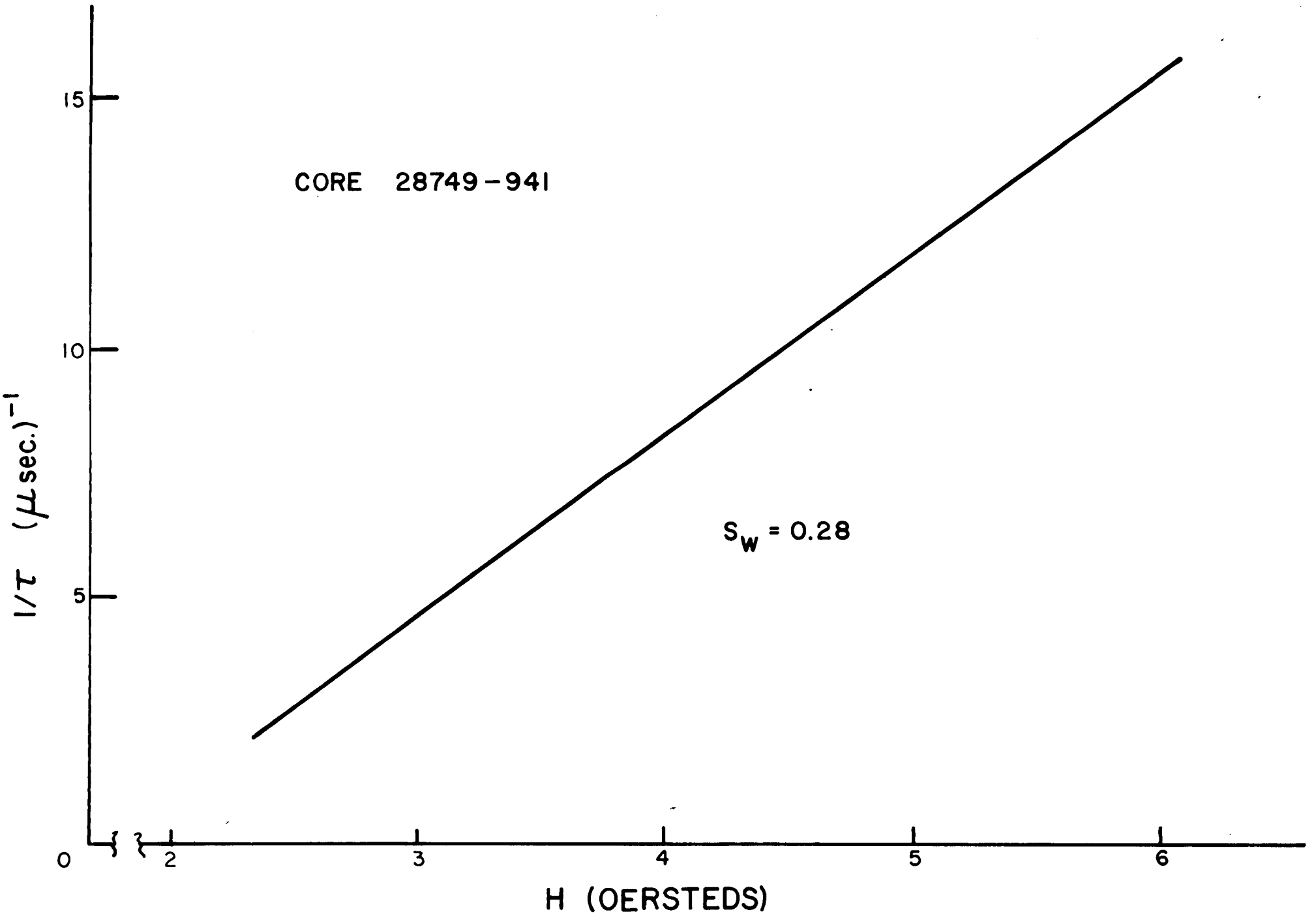
CORE 28749-941
S_w = 0.28
$1/\tau$ (μsec.)$^{-1}$
15
10
5
0
2
3
4
5
6
H (OERSTEDS)

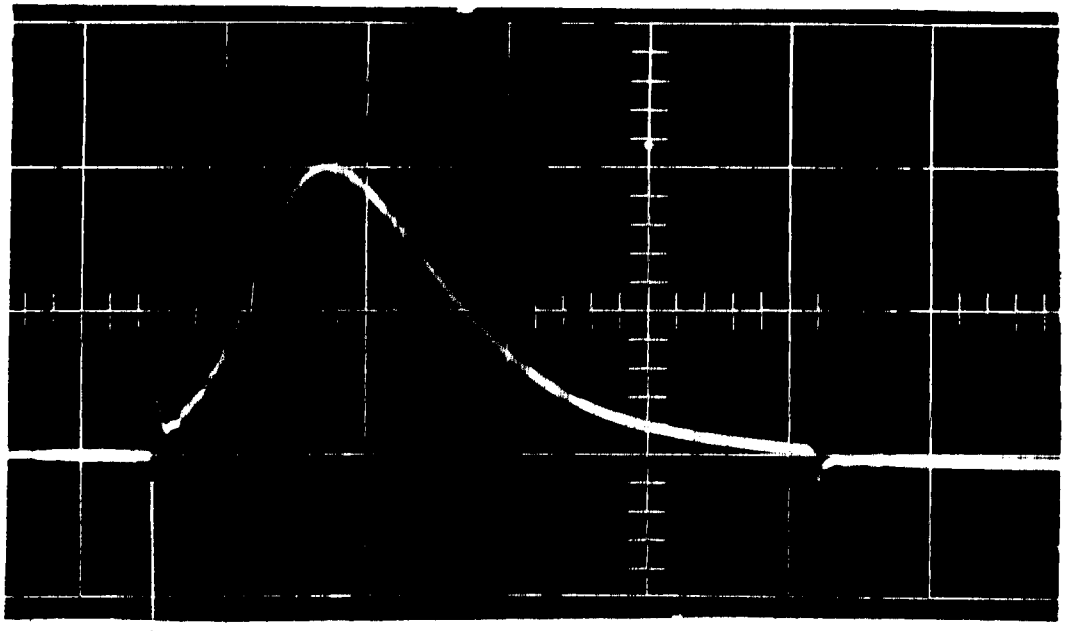

$\leftarrow \tau \rightarrow$

(0.35 μsec.)

TIME SCALE: 0.1 μsec./DIV.

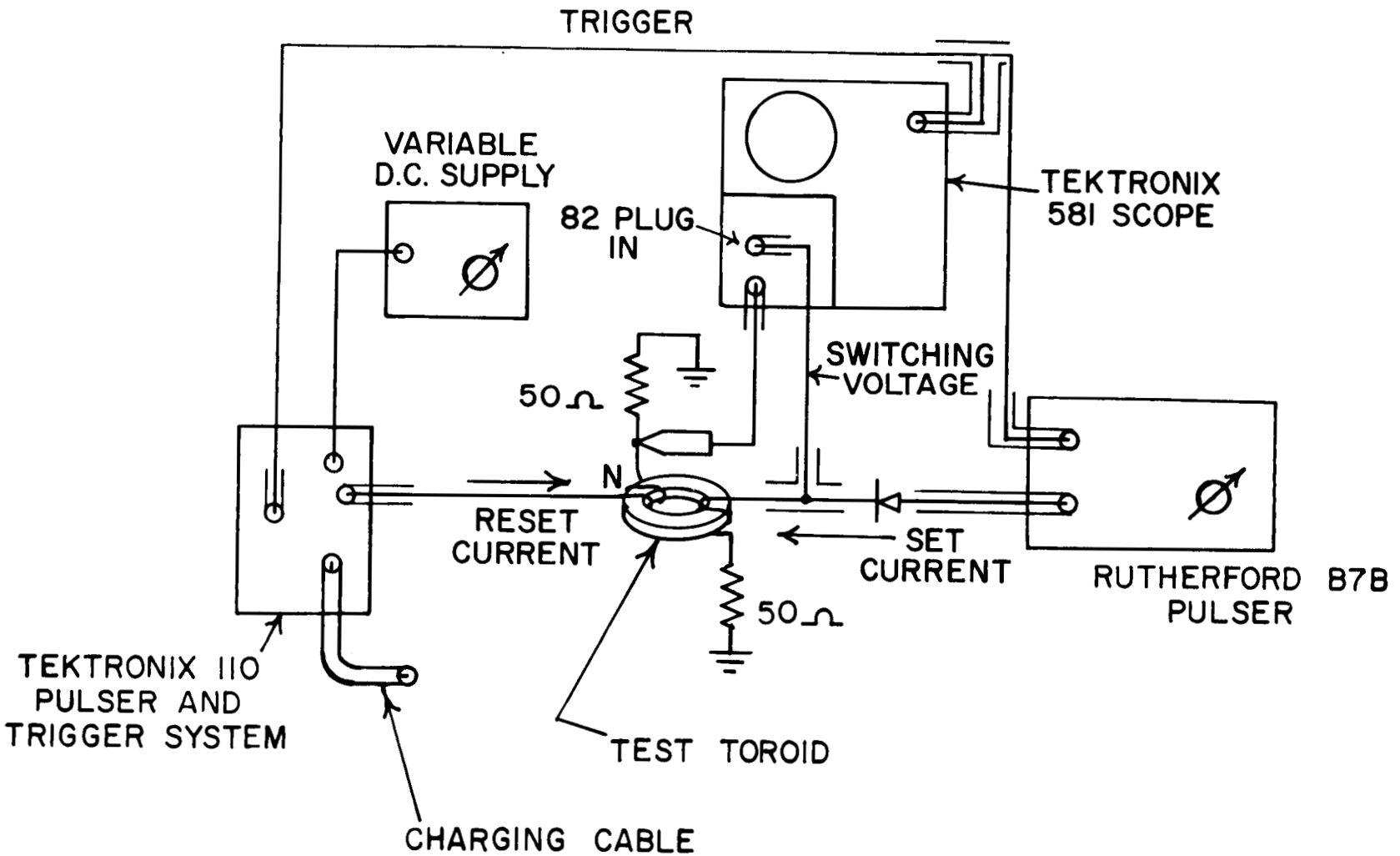
TRIGGER
VARIABLE
D.C. SUPPLY
82 PLUG
IN
TEKTRONIX
581 SCOPE
50 Ω
SWITCHING
VOLTAGE
N
RESET
CURRENT
SET
CURRENT
RUTHERFORD B78
PULSER
50 Ω
TEKTRONIX 110
PULSER AND
TRIGGER SYSTEM
TEST TOROID
CHARGING CABLE

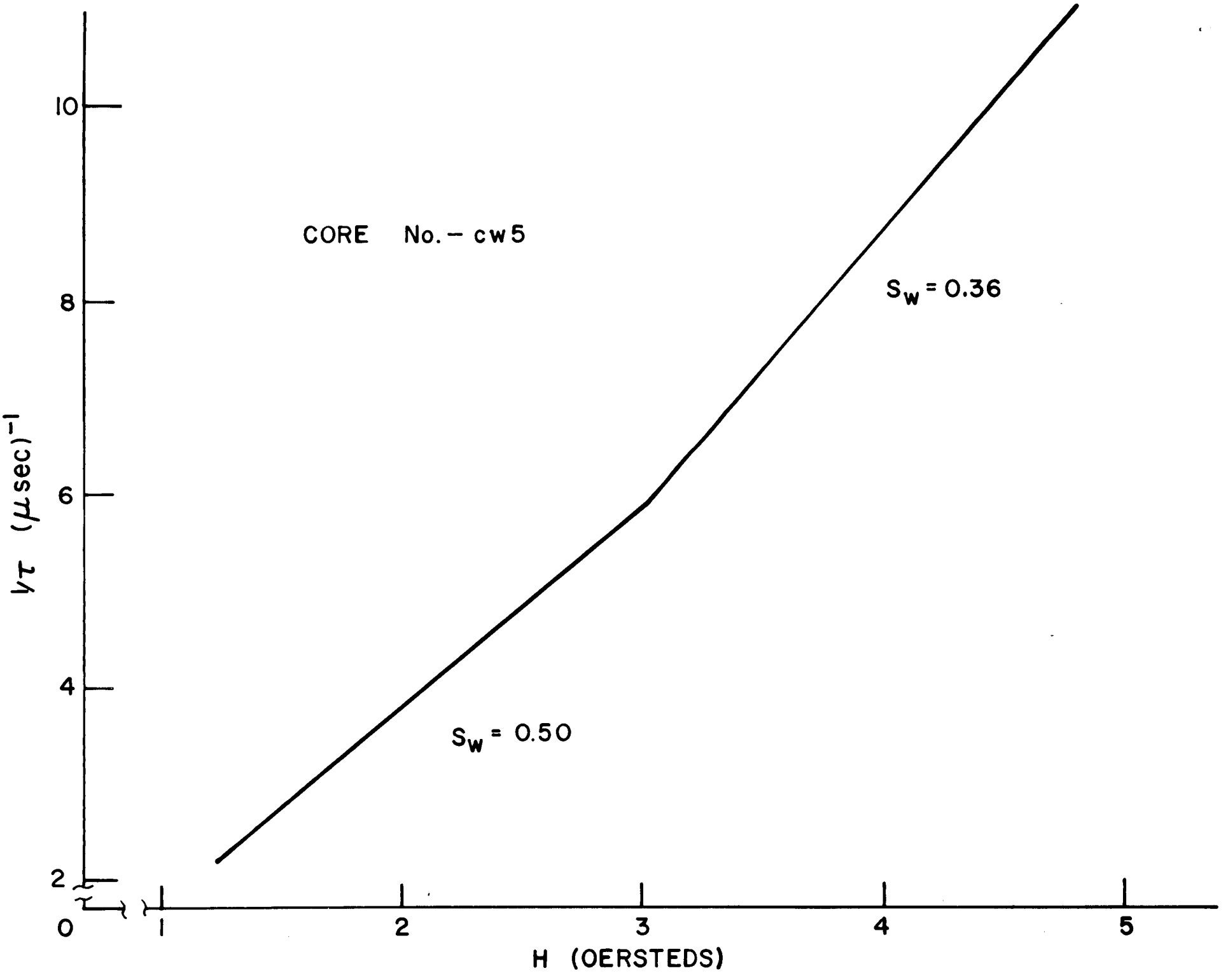
CORE No. – cw5
S_w = 0.36
S_w = 0.50
$1/\tau$ (μsec)$^{-1}$
H (OERSTEDS)
0
2
4
6
8
10
1
2
3
4
5

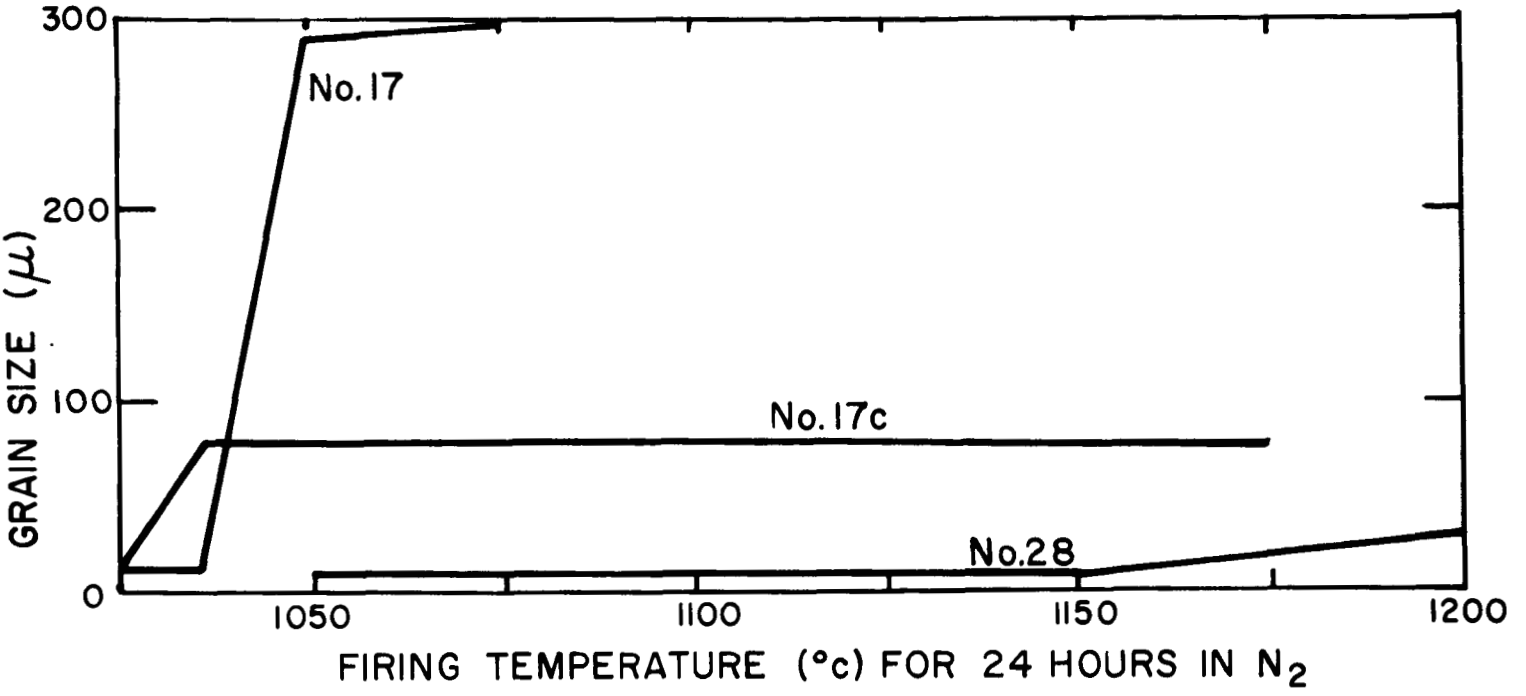
300
200
100
0
GRAIN SIZE (μ)
No. 17
No. 17c
No. 28
1050
1100
1150
1200
FIRING TEMPERATURE (°c) FOR 24 HOURS IN N_2

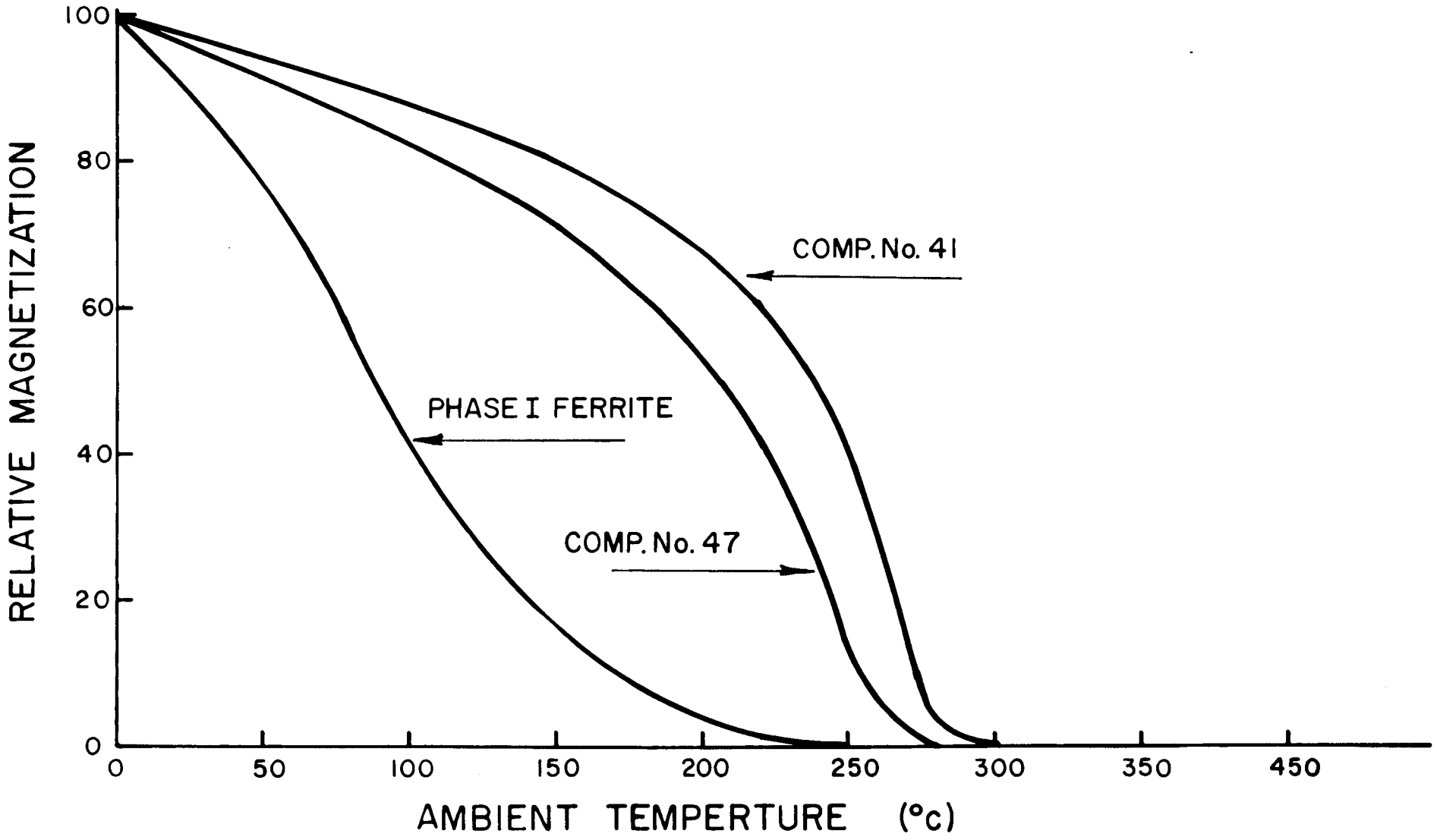
RELATIVE MAGNETIZATION
100
80
60
40
20
0
0
50
100
150
200
250
300
350
450
AMBIENT TEMPERTURE (°c)
COMP. No. 41
PHASE I FERRITE
COMP. No. 47

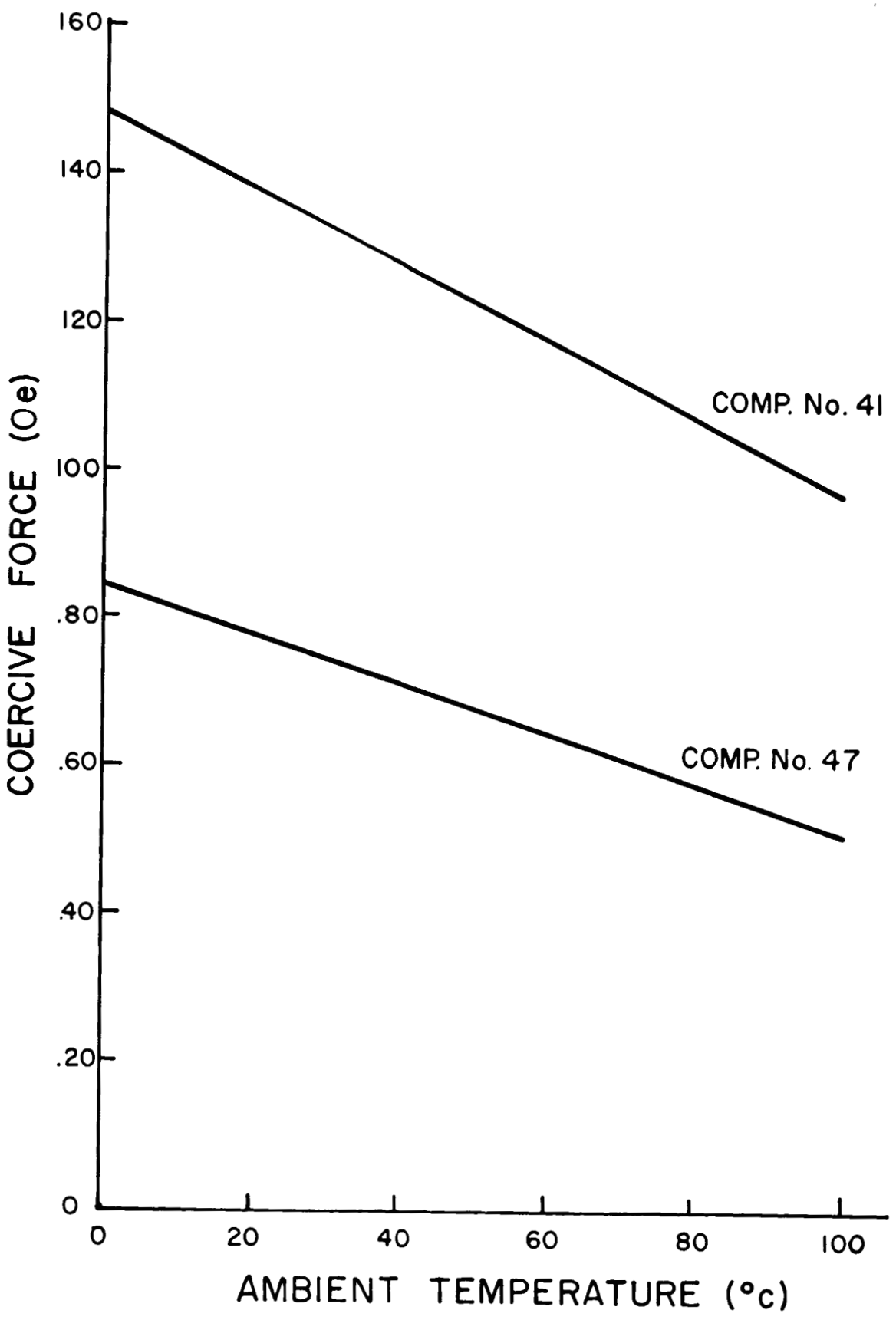
160
140
120
100
.80
.60
.40
.20
0
COERCIVE FORCE (Oe)
COMP. No. 41
COMP. No. 47
0
20
40
60
80
100
AMBIENT TEMPERATURE (°c)

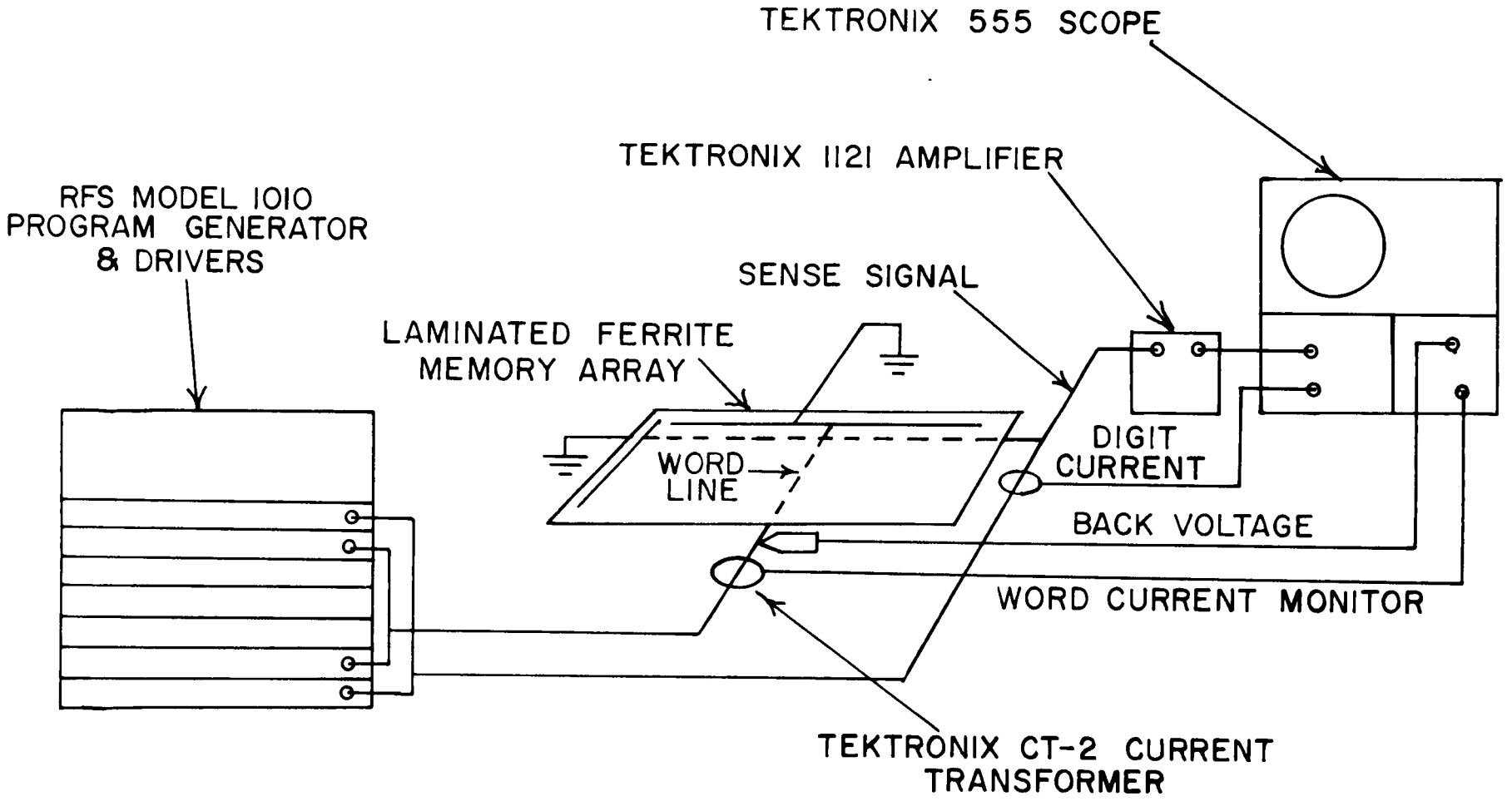
TEKTRONIX 555 SCOPE
TEKTRONIX 1121 AMPLIFIER
RFS MODEL 1010
PROGRAM GENERATOR
& DRIVERS
SENSE SIGNAL
LAMINATED FERRITE
MEMORY ARRAY
WORD
LINE
DIGIT
CURRENT
BACK VOLTAGE
WORD CURRENT MONITOR
TEKTRONIX CT-2 CURRENT
TRANSFORMER

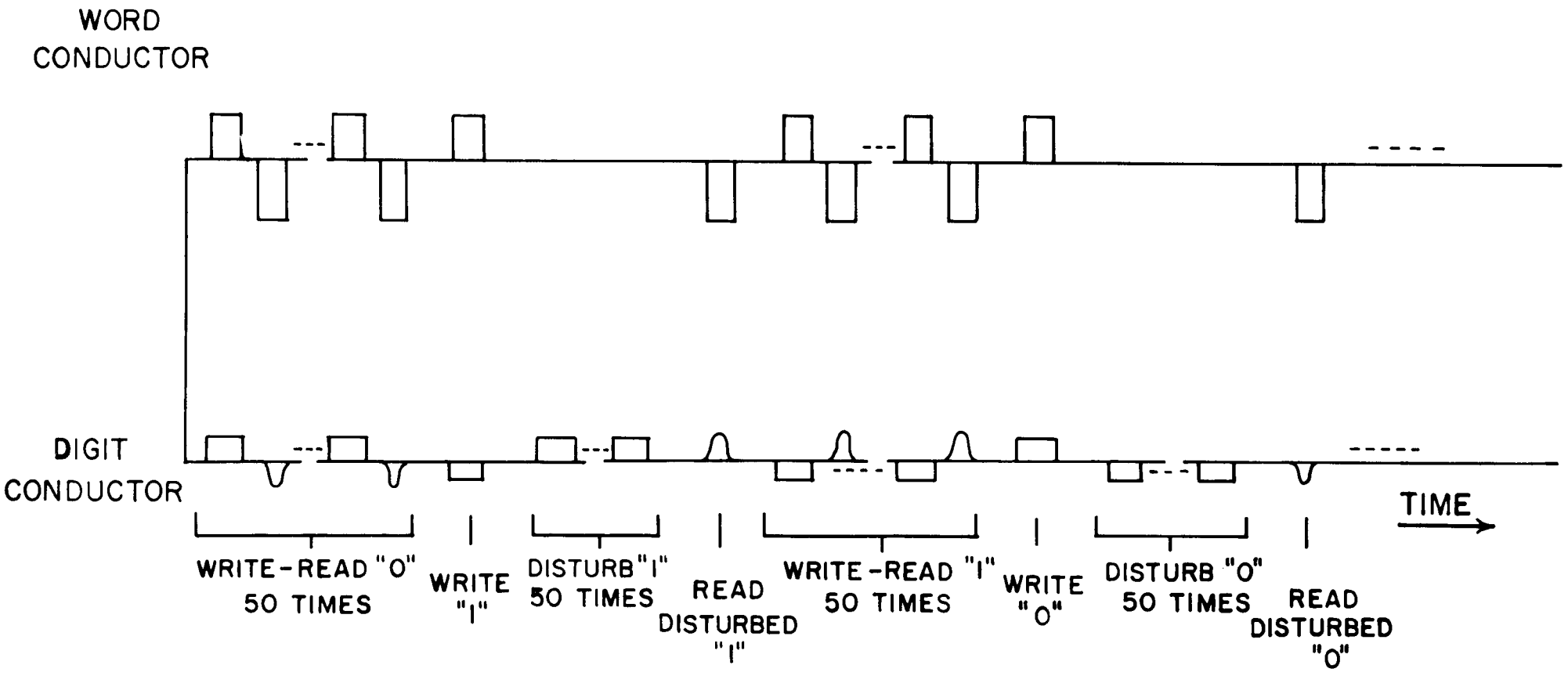
WORD
CONDUCTOR
DIGIT
CONDUCTOR
TIME
WRITE-READ "0"
50 TIMES
WRITE
"1"
DISTURB "1"
50 TIMES
READ
DISTURBED
"1"
WRITE-READ "1"
50 TIMES
WRITE
"0"
DISTURB "0"
50 TIMES
READ
DISTURBED
"0"

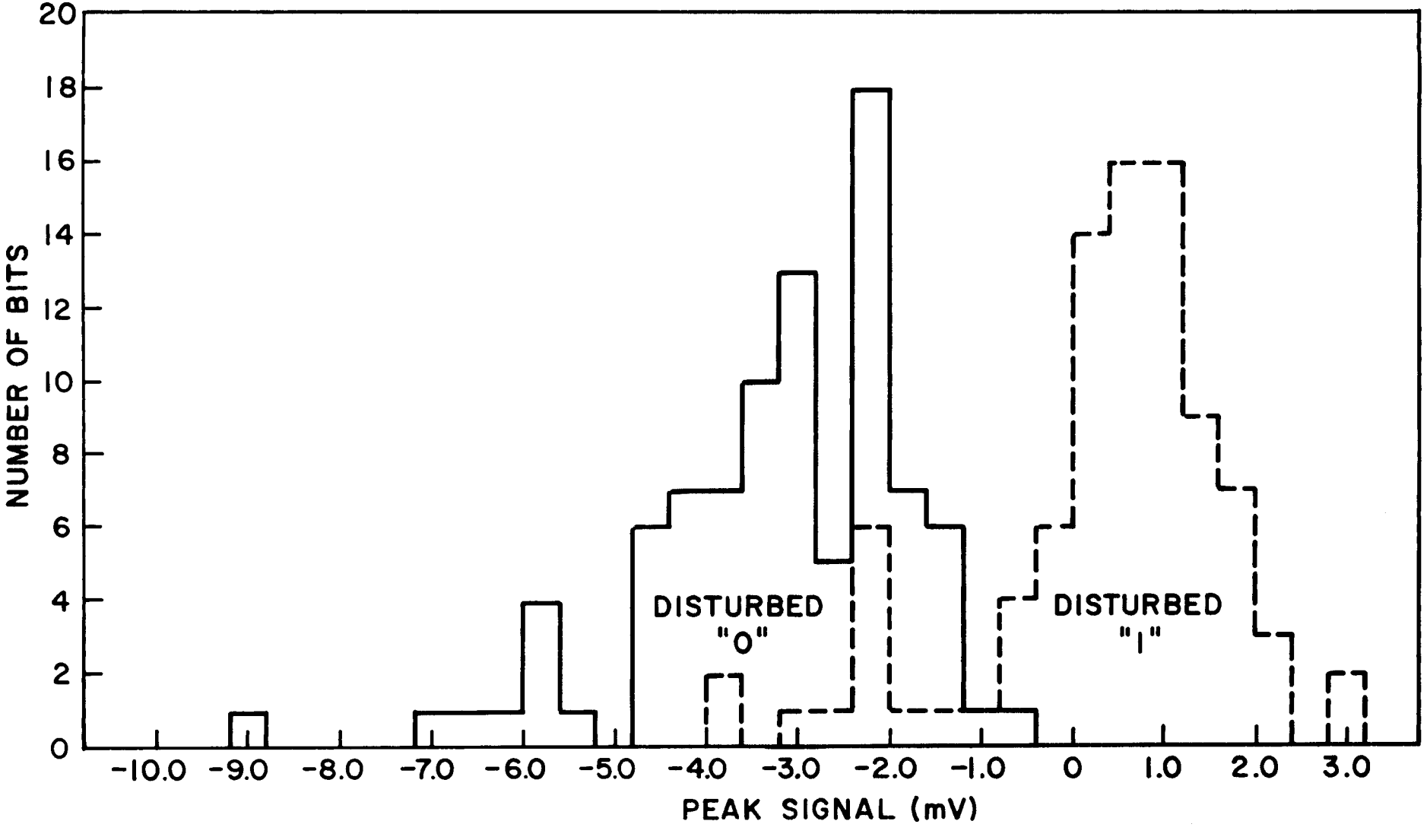
20
18
16
14
12
10
8
6
4
2
0
NUMBER OF BITS
DISTURBED
"0"
DISTURBED
"1"
-10.0
-9.0
-8.0
-7.0
-6.0
-5.0
-4.0
-3.0
-2.0
-1.0
0
1.0
2.0
3.0
PEAK SIGNAL (mV)

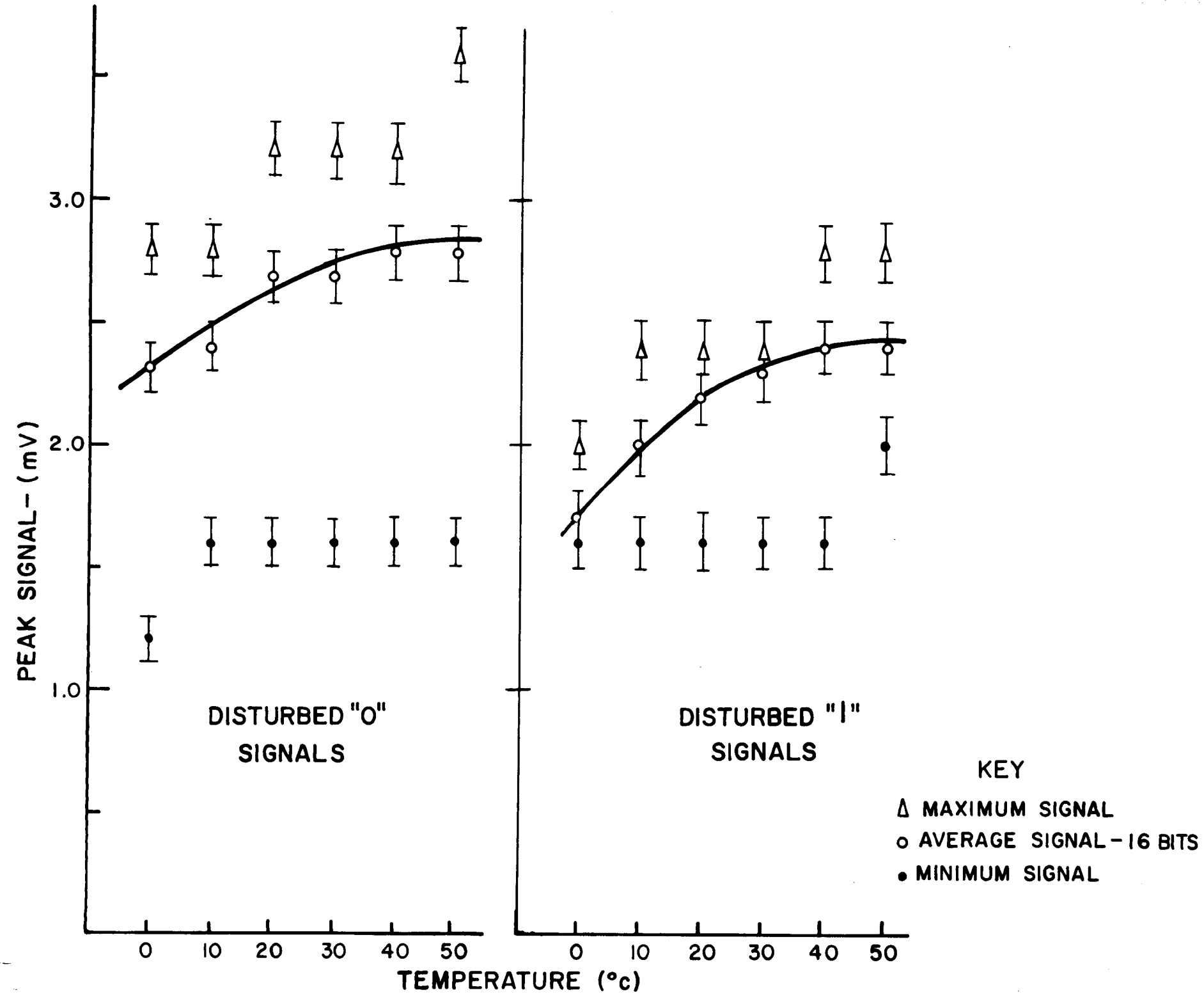
PEAK SIGNAL - (mV)
3.0
2.0
1.0
DISTURBED "0" SIGNALS
DISTURBED "1" SIGNALS
0
10
20
30
40
50
TEMPERATURE (°c)
KEY
Δ MAXIMUM SIGNAL
o AVERAGE SIGNAL - 16 BITS
• MINIMUM SIGNAL

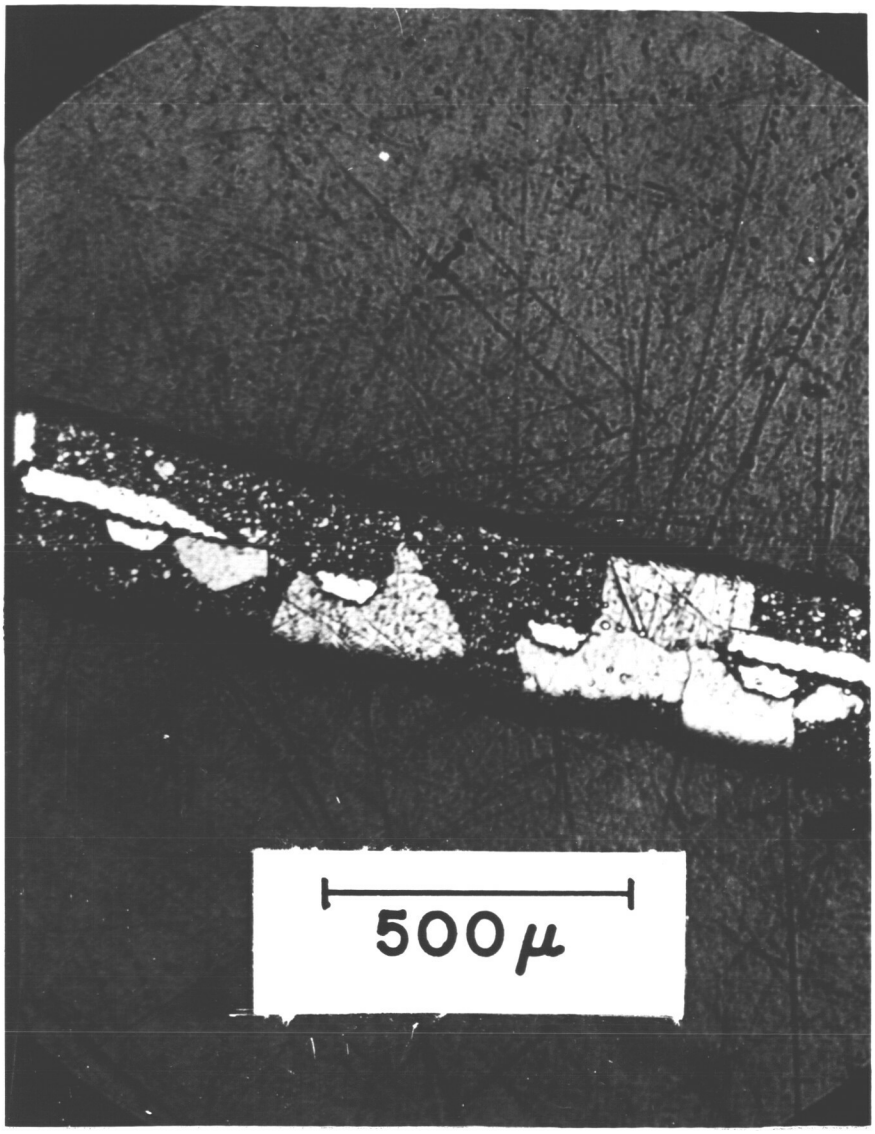
500 μ